Biophysical Journal
Article

Biophysical Society

Dynamics of Chromatin Fibers: Comparison of Monte Carlo Simulations with Force Spectroscopy

Davood Norouzi[1,*] and Victor B. Zhurkin[1,*]
[1]Laboratory of Cell Biology, CCR, National Cancer Institute, NIH, Bethesda, Maryland

ABSTRACT To elucidate conformational dynamics of chromatin fibers, we compared available force-spectroscopy measurements with extensive Monte Carlo simulations of nucleosome arrays under external force. Our coarse-grained model of chromatin includes phenomenological energy terms for the DNA-histone adhesion and the internucleosome stacking interactions. We found that the Monte Carlo fiber ensembles simulated with increasing degrees of DNA unwrapping and the stacking energy 8 kT can account for the intricate force-extension response observed experimentally. Our analysis shows that at low external forces ($F < 3.0$ picoNewtons), the DNA ends in nucleosomes breathe by ~10 bp. Importantly, under these conditions, the fiber is highly dynamic, exhibiting continuous unstacking-restacking transitions, allowing accessibility of transcription factors to DNA, while maintaining a relatively compact conformation. Of note, changing the stacking interaction by a few kT, an in silico way to mimic histone modifications, is sufficient to transform an open chromatin state into a compact fiber. The fibers are mostly two-start zigzag folds with rare occurrences of three- to five-start morphologies. The internucleosome stacking is lost during the linear response regime. At the higher forces exceeding 4 picoNewtons, the nucleosome unwrapping becomes stochastic and asymmetric, with one DNA arm opened by ~55 bp and the other arm only by ~10 bp. Importantly, this asymmetric unwrapping occurs for any kind of sequence, including the symmetric ones. Our analysis brings new, to our knowledge, insights in dynamics of chromatin modulated by histone epigenetic modifications and molecular motors such as RNA polymerase.

INTRODUCTION

The hierarchical organization of eukaryotic DNA into nucleosomes and higher-order structures has profound implications for DNA accessibility by regulatory factors. Nucleosome arrays present a barrier to DNA-binding proteins in two ways. First, the DNA fragments wrapped in nucleosomes are 145–147 bp (1,2), whereas the linkers are 15–80 bp long depending on the organism and cell type (3), indicating that more than two-thirds of the eukaryotic genome is sterically blocked by histones. The second obstacle is the chromatin compaction induced by internucleosome stacking interactions (4). It is widely accepted that posttranslational modifications of histone tails can alter these interactions and thereby change the level of compaction of chromatin and the DNA accessibility (5–9). Therefore, elucidating the structural details of conformational transitions in chromatin is one of the central problems in molecular cell biology.

One of the promising approaches to this problem is force spectroscopy, which allows for picoNewton (pN) manipulation and nanometer-precision measurements of single chromatin fibers under external force (10–17). However, the structural interpretation of the data at the subnucleosomal level remains elusive. For example, there are ongoing debates about the existence of regular stacked fiber arrays at low forces versus open unstacked conformations and solenoid versus zigzag geometries and whether the internucleosomal stacking plays a role or the unwrapping of DNA from histones can account for all the force-spectroscopy observations (10–19). To obtain structural information at the mononucleosomal level, an appropriate stereochemical model that adequately describes the known structural and dynamic characteristics of chromatin fibers is necessary.

Cui and Bustamante (10) were the first to analyze chromatin fiber stretching under external force, using optical tweezers. They interpreted the nonlinear force-extension curves as a transition between condensed and decondensed states of the fiber. Fitting their data by the worm-like chain polymer model, they estimated the internucleosome interaction energy, E, to be ~3 kT (in solution containing 40–150 mM NaCl). Unwrapping of nucleosomal DNA was not considered in their model. Kruithof et al. (13) used magnetic tweezers and the 601 nucleosome positioning sequence to probe the unfolding of chromatin at a higher

Submitted December 4, 2017, and accepted for publication June 19, 2018.
*Correspondence: davood.norouzi@nih.gov or zhurkin@nih.gov
Editor: Jason Kahn.
https://doi.org/10.1016/j.bpj.2018.06.032

resolution, particularly at small forces. They found that at forces up to $F \approx 3$ pN, the fiber stretches reversibly similar to a Hookean spring, whereas at force $F \approx 4$ pN, there is a plateau, hypothetically related to the unstacking of nucleosomes. Based on a two-state statistical-mechanical model of the fiber, a higher estimate for the stacking energy was suggested, $E \approx 14$ kT (in the presence of Mg^{2+} ions). It was proposed that a fiber with the nucleosome repeat length (NRL) 167 bp has the two-start "stiff" configuration, whereas NRL = 197 bp corresponds to a more flexible solenoid conformation. Later on, van Noort and co-workers (15) presented a more elaborate theoretical analysis of the force-extension curves. They estimated the stacking energy to be $E \approx 10$ kT, with ~30 bp DNA being unwrapped even at small forces.

However, the same experimental data were interpreted differently by other authors. For example, Victor et al. (18) explained both the linear and the plateau force regimes observed by Kruithof et al. (13) by gradual unwrapping of DNA, solely within the zigzag model of fiber morphology. Chien and van der Heijden (19) also suggested that the force plateau regime represents the unwrapping of DNA rather than the unstacking of nucleosomes. They put the upper limit $E \approx 1$ kT on the stacking interaction. This short overview demonstrates that the interpretation of force-extension data based on "simple" polymer models is quite ambiguous. In particular, the stacking energy estimates vary from $E \approx 1$ to 15 kT based on the same data. Clearly, a more sophisticated model of chromatin is required that is in accord with experimental observations and resolves more structural details.

Potentially, Monte Carlo (MC) simulations can shed light on the conformational dynamics of chromatin fibers, including force-induced chromatin unraveling. To span efficiently a structurally rich conformational space of oligonucleosomal arrays, various coarse-grained MC approaches have been employed (20–29). In particular, Collepardo-Guevara and Schlick (24) used an integrated chromatin coarse-grained model to analyze the role of dynamic-linker histone in chromatin fiber softening. However, because the ability of the nucleosomal DNA to peel off the histone was not included in this model, the simulated fiber extensions were noticeably less than those observed experimentally. Recently, Dobrovolskaia et al. (25) and Lequieu et al. (26) independently introduced coarse-grained models to investigate the dynamics of force-induced unwrapping of DNA in single nucleosomes. Kepper et al. (27) considered DNA unwrapping, and although their model adequately describes the inner-turn unwrapping of DNA at high forces, at small forces ($F < 6$ pN) their calculations overestimate the stretching response of the fiber measured experimentally.

Overall, the MC simulation studies published so far correctly reproduce certain parts of experimentally observed fiber unraveling but fail to describe the whole process precisely. Therefore, we found it necessary to perform a new round of systematic MC simulations of chromatin fibers under external force, especially in light of the recent high-resolution force-spectroscopy measurements revealing the dynamic unwrapping-rewrapping transitions in nucleosomes in great detail (11–16). These data indicate that the low-force extension brings about a gradual symmetric unwrapping of DNA, whereas at high forces, the unwrapping becomes stochastic and asymmetric, with one DNA arm opened much stronger than the other arm (16).

Here, we used the available data on the DNA unzipping dwell times (12) to elucidate a free-energy profile for unwrapping and from that analyze, in silico, the dynamic response of nucleosomal arrays to external force. We employed our coarse-grained model of chromatin fiber that has proven to be effective in predicting conformational and topological aspects of nucleosomal arrays with variable NRL (30). This approach allowed us to distinguish between unwrapping and unstacking of nucleosomes in different force regimes in agreement with experiments.

MATERIALS AND METHODS

We simulated nucleosome arrays consisting of 12 sequential nucleosome-linker units. The variable parameters of the system were the NRL and the DNA unwrapping, U, in bp, stacking energy E in kT, and external force F in pN. We used the template crystal structure of a nucleosome core particle with the Widom 601 DNA sequence resolved by x-ray crystallography (PDB: 3MVD (31)). This part was assumed to be fixed during simulations and only goes through rigid body motions except for the unwrapped DNA, which is treated as a part of the "dynamic" linker DNA. The linker DNA was modeled at the level of dimeric steps, and its trajectory was described by six base-pair step parameters (30,32). The geometry of the linker DNA fluctuates around the regular B-DNA. Note that a system of linker size L (NRL = 145 + L) and average unwrapping U has $6 \times (L + 2U + 1)$ degrees of freedom per nucleosome.

We used the following energy terms: elastic, electrostatic, histone H4 tail-acidic patch interactions, and the steric hindrance as we employed in a previous study (30). Moreover, the work done by the external force and changes in the adhesion energy of unwrapped DNA were added to the total energy (Fig. S1). Here are some details regarding the energy terms:

1) The elastic energy of the linker DNA deformations was calculated using a knowledge-based quadratic potential function (32).
2) The electrostatic energy was calculated using the Coulomb potential with a 30-Å cutoff. Positive charges on arginines and lysines, as well as negative charges on aspartates, glutamates, and DNA phosphates were considered. All charges were partially neutralized to mimic the salt screening effects.
3) Stacking or the H4 tail – acidic patch interactions were modeled phenomenologically, with the variable internucleosome interaction energy E and a 35-Å range of action (30).
4) Steric clashes were modeled by a van-der-Waals-like repulsion potential.
5) Work done by the external force F was calculated as $-F \times Z_{ext}$, where the last term is the fiber extension measured along the external force.
6) The DNA-histones adhesion energy was obtained by translating the DNA unzipping dwell times measured by Hall et al. (12) into the energy profile $G_{adh}(U)$ (Fig. S2).

For starting conformations, the DNA linkers were constructed randomly using the Gaussian sampling method (33). Afterward, the following MC steps were performed:

1) randomly selecting a DNA base-pair step in one of the "dynamic" linkers and alteration of its six parameters by adding a random perturbation,

2) updating positions of all nucleosomes in the nucleosome array, and
3) computing the energy difference and performance of the Metropolis acceptance test (34).

Every construct was simulated for 150 million MC steps for a given E and force F. The final 100 million MC steps were used for statistical averaging of various parameters of the system (e.g., average Z_{ext} and fraction of stacked nucleosomes). Two rounds of simulations were performed, first with constant unwrapping U and then with the dynamic unwrapping. The first round gave us a general idea on the level of the fiber extension that would match the experiment at each force regime. However, this approach does not reflect the asynchronous and stochastic nature of the nucleosome unwrapping. Therefore, in the second round, the DNA unwrapping was described by the independent parameters $U^L{}_i$ and $U^R{}_i$ representing the numbers of unwrapped basepairs at the left and right ends of nucleosome i. A snapshot of such a nucleosomal array is depicted in Fig. 1. Details of the fiber geometry, energy terms, and MC moves are given (Figs. S1–S3).

In the first round of simulations, fibers with unwrapping $U = 0, 5, \ldots, 60$, and 72 bp (free DNA) and stacking energy $E = 0$, 6, 8, 10, and 12 kT were analyzed. In all cases, the force was varied from 0 to 8 pN with steps of 0.5 pN. We found that the best fit of the force-extension data was obtained for $E = 8$ kT. This stacking energy was used in the second round of simulations with stochastic unwrapping of nucleosomes. Overall, ~3000 simulations (3000 × 150 million MC steps) were performed on the National Institutes of Health supercomputer cluster, Biowulf.

Compactness of the chromatin and distribution of internucleosomal distances are important characteristics describing the geometry of a fiber. We measured the level of compaction by the average stacked fraction (SF) of nucleosomes in a fiber. The SF was calculated by dividing the total stacking energy to the maximal possible stacking energy for each MC snapshot. We also calculated the frequency of internucleosome interactions (FINI) in our MC ensembles. This value represents nearest-neighbor interactions along the chromatin fiber. To calculate the FINI, two nucleosomes i and i+n are considered to be in contact if the center-to-center distance is less than 120 Å. Total contacts are normalized to all possible neighbors with distance n along the fiber. These contact map profiles provide important information regarding the fiber morphology.

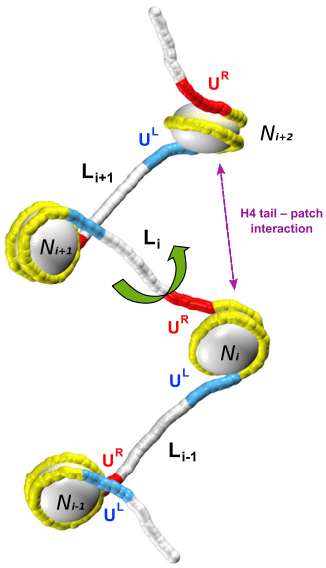

FIGURE 1 Schematic presentation of a nucleosome array and the variable parameters of the system. The DNA unwrapping is described by parameters U^L and U^R representing the numbers of unwrapped basepairs at the left and right ends of nucleosomes. (The U^L and U^R values are changing independently in each nucleosome.) The static histone cores are shown by the white beads and the static wrapped DNA is shown in yellow, whereas the dynamic linkers are shown as white, blue, and red tubes. In a single MC step, a dynamic linker L_i (connecting nucleosomes N_i and N_{i+1}) is chosen. Then, in this linker, a dimeric step is selected for modification (*green arrow*). Details of the fiber geometry, energy terms, and MC moves are given in Figs. S1–S3. To see this figure in color, go online.

RESULTS

In this study, we compared extensive MC simulations with the force-spectroscopy measurements reported by Meng et al. (15), who employed DNA vectors with inserts containing 30 × 167 and 15 × 197 bp repeats of the Widom 601 nucleosome positioning sequence. Extracting the force-extension response of the nucleosome arrays from raw experimental data is explained in Fig. S4. The adjusted experimental data are presented in Fig. 2 as thick solid lines. For the MC simulations, first we analyzed the role of the uniform DNA unwrapping in the fiber stretching in the absence of stacking interactions ($E = 0$). Then, we investigated how changes in the internucleosome stacking energy, E, influence the force-extension maps of the fibers. Comparison of the Meng et al. (15) data with MC simulations revealed a consistent picture of unstacking and unwrapping of nucleosomes as a function of external force. Furthermore, our simulations are in agreement with the stochastic asymmetric unwrapping of nucleosomes observed by Ngo et al. (16).

Role of nucleosome unwrapping in the fiber stretching

The experimental and MC-simulated force-extension (F, Z_{ext}) responses are presented in Figs. 2 and S5. The experimental curves are naturally divided into the following three regions:

The left shoulder, with forces less than 3 pN

The MC-simulated curves demonstrate a linear force-extension dependence for small uniform unwrapping $U \leq 12$ bp in this regime. Importantly, the inclination of the MC curves for U ~10 bp are close to that of the experimental curves (for both NRL = 167 and 197 bp). Of note, the slope of the (F, Z_{ext}) curve (or stretching stiffness of the fiber) strongly depends on the nucleosome spacing: the stiffness is 0.65 pN/nm for NRL = 167 bp and 0.3 pN/nm for NRL = 197 bp, in close agreement with experimental data. Therefore, the experimentally observed linear response is not necessarily an indication of a fully stacked fiber as proposed earlier (15,17).

The plateau region, with intermediate forces F = 3–4 pN

The left and right boundaries of the plateau approximately correspond to $U = 10$ and 25 bp. Here, inclinations of the experimental force-extension curves are close to zero, indicating significant fiber stretching under the constant load.

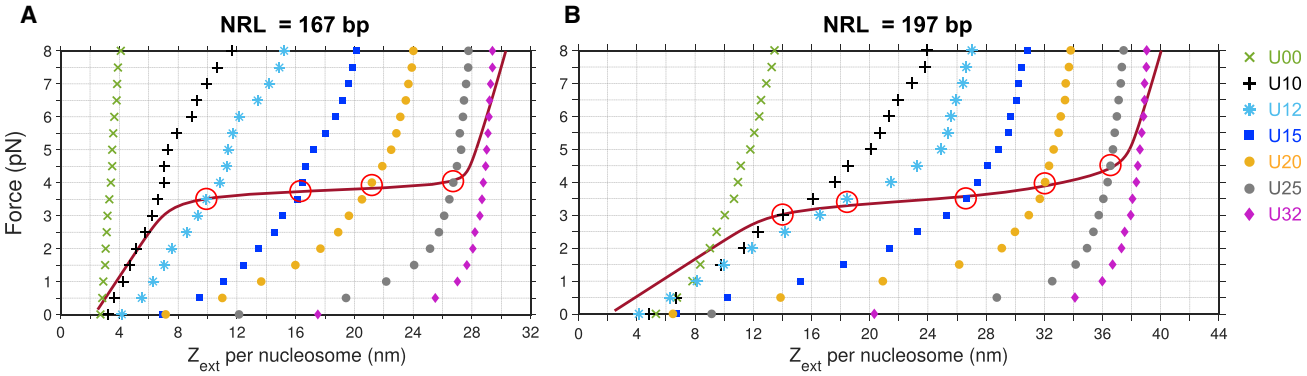

FIGURE 2 Force-extension profiles for fibers with NRL = 167 bp (*A*) and 197 bp (*B*) for various degrees of unwrapping of nucleosomes, *U*, varying from 0 to 32 bp, with stacking energy $E = 0$. The symbols represent the average extension per nucleosome obtained from MC simulations. The solid curves represent experimental data (15). The circles indicate the points of intersection of the MC curves with the experimental (F, Z_{ext}) curves in the central plateau region. Simulations were performed for forces from 0 to 8 pN in steps of 0.5 pN. The standard deviation (SD) of the extension, Z_{ext}, is ~1 nm at low forces; it shrinks below 0.2 nm at high forces. Curves for $U = 5$, 60 bp, and free DNA are presented in Fig. S5. To see this figure in color, go online.

The MC curves intersect the experimental (F, Z_{ext}) curves in the central plateau region (see the *circles* in Fig. 2). Remarkably, the increase in fiber extension in the plateau region is nearly the same, $\Delta Z_{ext} = 20 \pm 2$ nm, for NRL = 167 and 197 bp, which is in accord with equal unwrapping of nucleosomal DNA in these two cases. This requires that at this level of fiber extension ($Z_{ext} >$ 10–15 nm for NRL = 167–197 bp, respectively) the internucleosome stacking is lost. Figs. 3 and S6 represent the stretched conformations simulated at $E = 8$ kT. They show that before the plateau force ($F \approx 3.5$ pN) all internucleosomal stacks disappear.

The right shoulder, with forces higher than 4 pN

The experimental curves display a "steep" inclination at $F > 4.0$ pN. The severely extended conformations of the fiber at these forces indicate a significant unwrapping of nucleosomal DNA by $U = 25$–32 bp, which corresponds to a complete unfolding of the outer-turn DNA (Fig. 4 *A*). Notably, for $U \geq 25$ bp, the force-extension curves behave similar to a semiflexible polymer. The MC curves for $U = 25$–72 bp can be fitted by the worm-like chain model with the persistence length ranging from 20 to 70 nm (Fig. S5).

The structural details of the fiber extension become clear from analysis of the nucleosome end-to-end distance as a function of unwrapping *U*, or end-to-end distance Dist(*U*) (Fig. 4 *B*). Indeed, the slope of the Dist(*U*) curve is the highest in the interval $U = 10$–25 bp. Here, unwrapping of the nucleosome by 10 bp brings about an increase in the end-to-end distance of ~8 nm, whereas at the left and right ends of the Dist(*U*) plot, the same unwrapping produces an increase of only ~2 nm. The Dist(*U*) dependence can be explained qualitatively by comparing trajectories of the partially unfolded nucleosomal DNA (Fig. 4 *A*). When unwrapping increases from $U = 10$ to 25–32 bp, the angle between the DNA linkers (or the end vectors) increases from zero to ~180°; accordingly, the nucleosome end-to-end distance (and the total length of the fiber) also significantly increases. Earlier, similar unfolding geometries were reported for single nucleosomes under external tension (25,26,35). Overall, these geometric considerations provide a simple structural explanation of the nonlinear relationship between fiber stretching, Z_{ext}, and unwrapping of DNA in nucleosomes, *U* (Fig. 2).

Internucleosome stacking and fiber stretching

As shown in the previous section, the increasing unwrapping accompanying an increase in external force appears to explain most of the experimental observations. However, there is a discrepancy between our MC simulations and experimental results for NRL = 197 bp at the small force regime; MC simulations predict a more extended fiber than the experiments demonstrate. For example, at $F = 1$ pN, MC predicts an average extension $Z_{ext} \approx 8.0$ nm, whereas the experiment shows a ~6.0 nm extension (Fig. 2 *B*). This difference might be an indication of the attractive stacking interactions that force the fiber to shrink.

Therefore, we systematically changed the stacking energy *E* from 0 to 12 kT and unwrapping *U* up to 15 bp (for both NRL = 167 and 197 bp); see Fig. S7. (The values $U > 15$ bp are excluded from consideration, because they do not show a stable linear behavior at small forces.) Overall, the stretching behavior of the fibers is characterized by two "natural" trends: unwrapping makes a fiber more flexible and leads to more extended conformations, whereas an increase in stacking interaction makes a fiber stiffer and reduces the length of the fiber. As follows from the force-extension curves presented in Fig. S7, the stacking energy $E \approx 8$ kT can reproduce the experimentally observed extension of the chromatin fiber.

Dynamic unwrapping of nucleosomes

Until now, we assumed that the DNA unwrapping (described by the model parameter *U*) is the same in all

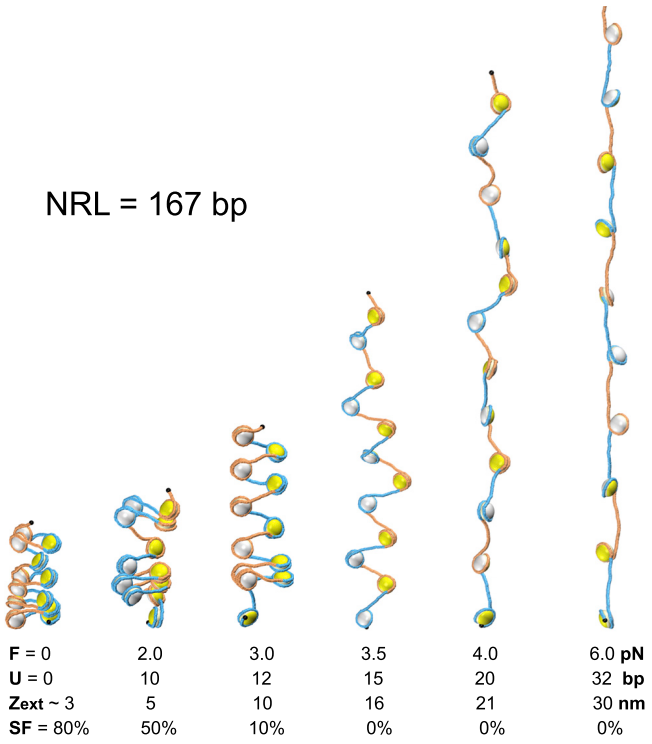

FIGURE 3 Typical conformations of chromatin fiber with NRL = 167 bp simulated for external forces increasing from 0 to 8 pN. Our comparative analysis reveals that at small forces, $F \leq 3.0$ pN, the DNA unwrapping is insignificant, $U \leq 12$ bp, and the fiber remains relatively compact despite numerous stacking-unstacking events. With an increase in applied force, the unwrapping of nucleosomal DNA becomes more pronounced and increases to $U = 20$ bp at $F = 4$ pN and up to $U = 32$ bp at $F = 8$ pN. These MC simulations were performed for stacking energy $E = 8$ kT. Note, however, that for $F = 3.5$ pN and higher, the internucleosome stacking is lost completely, and therefore, the results do not depend on the E value. The force-unwrapping, force-extension, and force-unstacking dependencies are presented at the bottom. Fiber conformations for NRL = 197 bp are presented in Fig. S6 (see also the Video S1 and S2). To see this figure in color, go online.

nucleosomes. However, the DNA unwrapping is a stochastic process (16,36,37). To take this into account, we considered a more sophisticated model with independent unwrapping of DNA at the left and right ends of each nucleosome and the DNA-histones adhesion energy, $G_{adh}(U)$, calculated as described in the Supporting Materials and Methods.

Before proceeding to the results of these simulations, note that according to the unzipping experiments by Hall et al. (12), the DNA-histone interactions are the strongest at positions 15–25 bp from the nucleosome ends and at positions 55–73 bp (that is, close to the nucleosome dyad), with relatively weak interactions in other regions of nucleosomal DNA. Accordingly, the adhesion energy function (modeling these interactions) has a nonlinear profile (Fig. S2). As shown below, this is important for understanding the dynamic unwrapping of nucleosomal DNA.

The force-extension dependencies obtained in these simulations are generally consistent with the experimental data, for both NRL = 167 and 197 bp (Fig. 5, *A* and *B*). Note, in particular, that the largest increase in Z_{ext} is observed in the plateau region, where changes in the fiber extension are the strongest according to the Meng et al. (15) measurements. At small forces, $F \leq 3.0$ pN, the average unwrapping (U^L and U^R) changes from 8 to 12 bp (Fig. 5, *C* and *D*). These values are very close to our estimates based on the uniform unwrapping simulations (Figs. 2 and S7, C and D).

At force $F = 4.0$ pN, we observed an abrupt change in DNA unwrapping. As shown in Fig. 5, *C* and *D*, the values U^L and U^R split into two branches, with $U \approx 8$ and 54 bp. Both U^L and U^R values are equally likely to be in the top and bottom branches; therefore, for $F = 4.0$ pN and higher, we used gray symbols (instead of *red* or *blue*). Additional details of this bifurcation are presented in Figs. S2 and S8. The main result is that at forces $F \geq 4.0$ pN, the distribution of DNA unwrapping becomes bimodal, with one peak corresponding to the U^L and U^R values ~10 bp and the second peak corresponding to a significant unwrapping of 55 (± 10) bp. The bimodal distribution of DNA unwrapping ($U^L \neq U^R$) helps decrease the total adhesion energy under strong tension. (For example, it is more favorable to have a strong unwrapping $U \approx 55$ bp at one end, rather than to have intermediate unwrapping $U \approx 30$ bp at the both ends of a nucleosome). Also, note that the asymmetrically unwrapped nucleosomes have Z_{ext} values comparable to the symmetric structure (Fig. 4 *A*). Therefore, the amount of work done by the external force is similar for the symmetric and asymmetric unwrapping. In turn, the observed bimodality is a consequence of the specific shape of the adhesion energy profile, namely, its downward curvature at $U \approx 25$ bp (Fig. S2). Importantly, there is no cooperativity in asymmetric unwrapping of neighboring nucleosomes, that is, the left and right arms of adjacent nucleosomes unwrap independently.

Probably, the most unexpected observation is that at high forces, the nucleosomes' spontaneous unwrapping occurs asymmetrically despite their intrinsically symmetric structure (we did not consider sequence asymmetries in our computations). These results are consistent with the fluorescence force-spectroscopy measurements by Ngo et al. (16) for the quasisymmetric sequence 601RTA. Using single-molecule fluorescence resonance energy transfer spectroscopy at force $F = 5$–15 pN, they observe considerable unwrapping at one end of nucleosome, whereas the other end remains (almost) fully wrapped. The probability of opening is equal for both sides of nucleosome 601RTA when averaged over many experimental traces, but in each individual trace, only one end is open. These observations may have profound consequences for the regulation of transcription.

Dynamic stacking of nucleosomes in the linear force regime

We found that the nucleosome arrays are not fully stacked in MC-simulated fibers. Because of thermal fluctuations, a

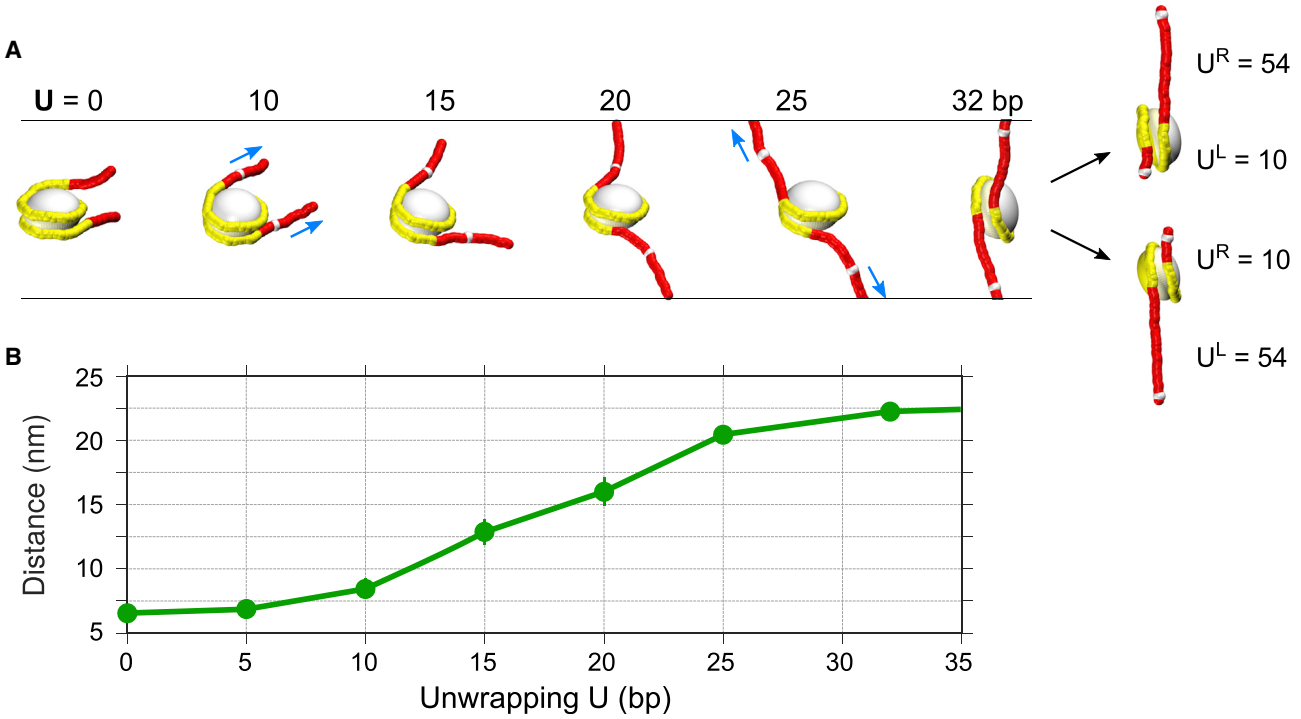

FIGURE 4 Gradual unwrapping of nucleosomes facilitates fiber stretching. (*A*) Typical conformations of nucleosomes in extended fibers. For unwrapping $U = 0$, all nucleosomal DNA is attached to histones (shown in *yellow*). For $U > 0$, the unwrapped DNA is represented by the red fragments located between the ends of the yellow fragments and the white markers (NCP positions 1 and 145). An increase in U brings about an increase in the angle between the DNA end vectors (*arrows* starting at the *white markers*) so that for $U = 25$–32 bp, this angle is ~180°, with the end vectors perfectly aligned along the external force. The alternative asymmetric conformations on the right, with U^L and U^R equal to 10 or 54 bp, have the same average degree of unwrapping as the $U = 32$ bp case and generate the same level of extension (Z_{ext}). However, the form of the adhesion energy profile and the stochastic dynamic of unwrapping-rewrapping dictates that these asymmetric conformations are preferable (Figs. 5 and S8). (*B*) The nucleosome end-to-end distance (between the *white markers* in (*A*)) as a function of unwrapping, U. The largest increase in this distance occurs between $U = 10$ and 25 bp, which roughly corresponds to the plateau limits (Fig. 2). To see this figure in color, go online.

significant number of nucleosome stacks are broken at $E = 8$ kT, even in the absence of external force (Fig. 5, *E* and *F*). An increase in the external force leads to a rapid, sigmoidal decrease in the SF of nucleosomes. A similar sigmoidal type of behavior was predicted by Meng et al. (15) based on a multistate statistical mechanical modeling of chromatin stretching (see *blue curve* in Fig. 5 *F*). However, it is assumed in the cited model that the fiber remains in a regular, fully stacked configuration during the linear phase of extension. The transition from a fully stacked to a fully unstacked fiber occurs at the plateau force $F \approx 3.5$ pN according to their model (13,15). Our MC simulations, without any assumption on the fiber regularity, indicate that sigmoidal transition occurs at smaller forces ($F \approx 3.0$ pN), and all nucleosome stacks are disrupted before the plateau force regime begins. Thus, according to our computations, the plateau region represents unwrapping and not unstacking of nucleosomes (for $E = 8$ kT, faithfully reproducing the experimental data (15)). If, however, the stacking energy is increased to $E = 12$ kT, the fibers remain fully stacked up to forces ~2.0 pN (Fig. S9), and the plateau level can exceed 4 pN (Fig. S7, E and G).

In summary, our results strongly suggest that the linear response (observed for the *left* shoulder of the force-extension curve) does not necessarily mean that nucleosomes are fully stacked in this regime (15). The more recent data on the fibers with the histone H4 tails cross-linked to the H2A acidic patches (17) are also compatible with the dynamic stacking model described here. It is highly likely that upon cross-linking, certain amounts of stacking interactions become permanent, whereas the fiber as a whole remains partially unstacked.

Simulation trajectories

The highly dynamic nature of nucleosome arrays, in simulations with $E = 8$ kT, is shown in the MC trajectories presented in Fig. 6. Whereas the total energy equilibrates quickly, variations in structural parameters such as the SF of nucleosomes and extension per nucleosome, Z_{ext}, remain significant. This means the equilibrium comprises multiple stacking-unstacking transitions at small forces. In other words, fiber is neither completely stacked nor completely open at all times. Examples of such half-open structures are given in Fig. 6. Note that the averages of U^L, U^R, and

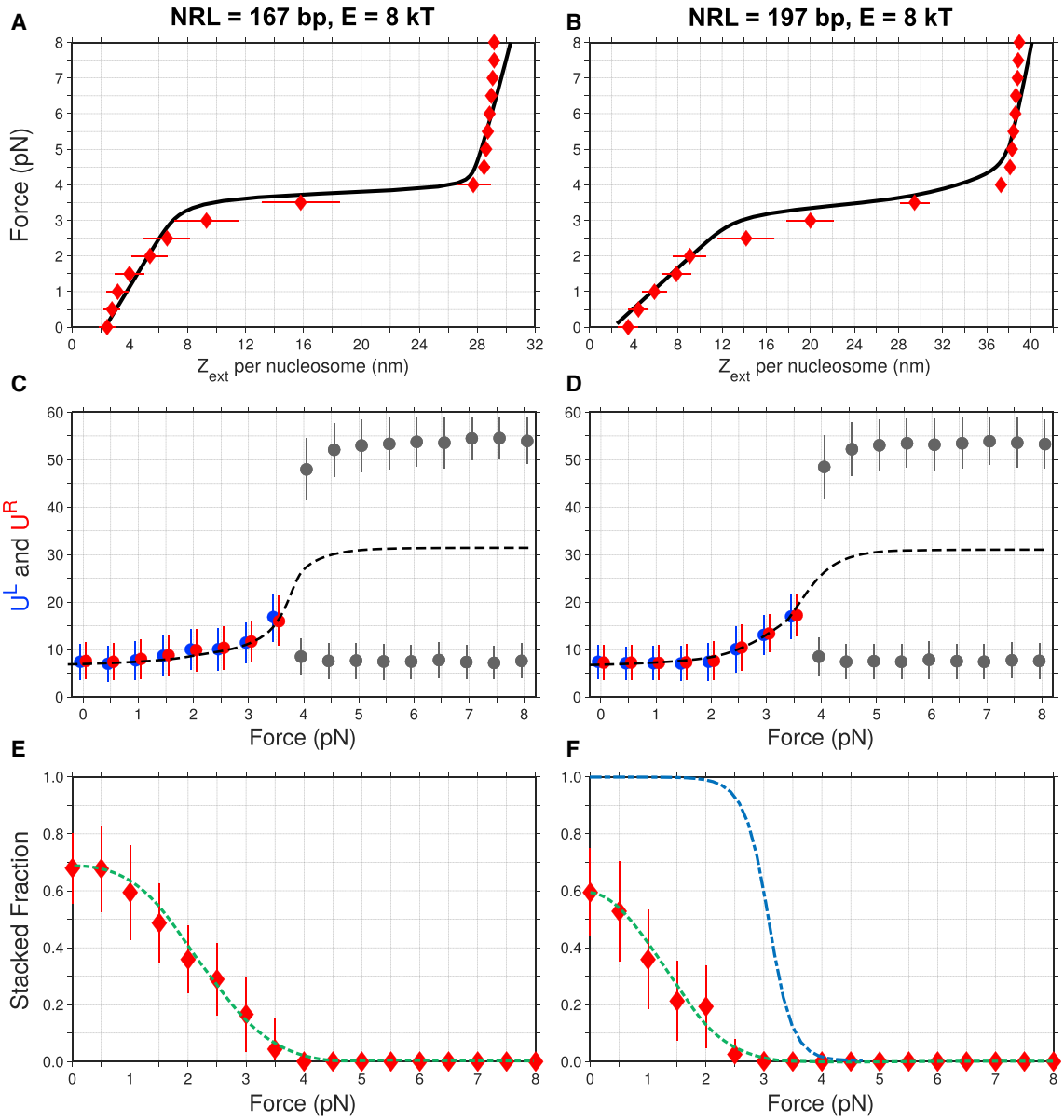

FIGURE 5 Response of the nucleosomal arrays (extension, unwrapping, and stacked fraction (SF)) to the external force. (*A* and *B*) The MC force-extension profiles (*red diamonds*) were calculated using the adhesion potential, $G_{adh}(U)$, for DNA unwrapping (Fig. S2) and $E = 8$ kT for stacking interactions. Note that the linear response persists up to $F = 2.0$–2.5 pN in both cases. The solid curves represent the adjusted experimental data (15). (*C* and *D*) DNA unwrapping at the left and right ends of nucleosomes (U^L in *blue* and U^R in *red*) is shown as a function of force. The average values are shown as circles, and SDs are shown as bars. As the external force increases from 0 to 3 pN, the DNA unwrapping (U^L and U^R) gradually changes from 8 to 12 bp, with an SD ~4 bp. These values are the averages over all 12 nucleosomes in the array and are in accord with our findings for the uniform U values (Figs. 2 and S7). At $F \geq 4.0$ pN, the DNA unwrapping undergoes bifurcation into two branches with $U \approx 8$ and 54 bp. Here, the circles and bars are shown in gray (i.e., not in *red* or *blue*), because asymmetric unwrapping occurs stochastically, that is, on average the chances of each nucleosome end (U^L or U^R) to be strongly unwrapped are equal (see Figs. S2 and S8 for details). The dashed curves represent the average unwrapping for both nucleosomal ends and exhibit a sigmoidal trend. (*E* and *F*) Average SFs of nucleosomes in fibers are shown as a function of force. Stacking energy is $E = 8$ kT. The sigmoidal blue curve is a result of statistical-mechanical modeling by Meng et al. (Fig. 3 *D* in (15)). The dashed green curves are sigmoidal fits over the MC results. Note that we do not observe a fully stacked fiber (SF = 1) at any force. To see this figure in color, go online.

Z_{ext} demonstrate a remarkable stability in equilibrium, despite wide variations in the SF of nucleosomes, from SF = 0 to 0.7 (Fig. 6). The SD of extension per nucleosome, Z_{ext}, is ~1.0 nm, or ~20% of the average value at small forces, comparable to fluctuations observed in experiment (Fig. S4). It is notable that stacking-unstacking fluctuations do not produce any detectable stepwise extensions (Fig. 6). In addition, the U^L and U^R variations, averaged over 12 nucleosomes in the array, are presented in this figure. Similar traces for higher forces, the average unwrapping

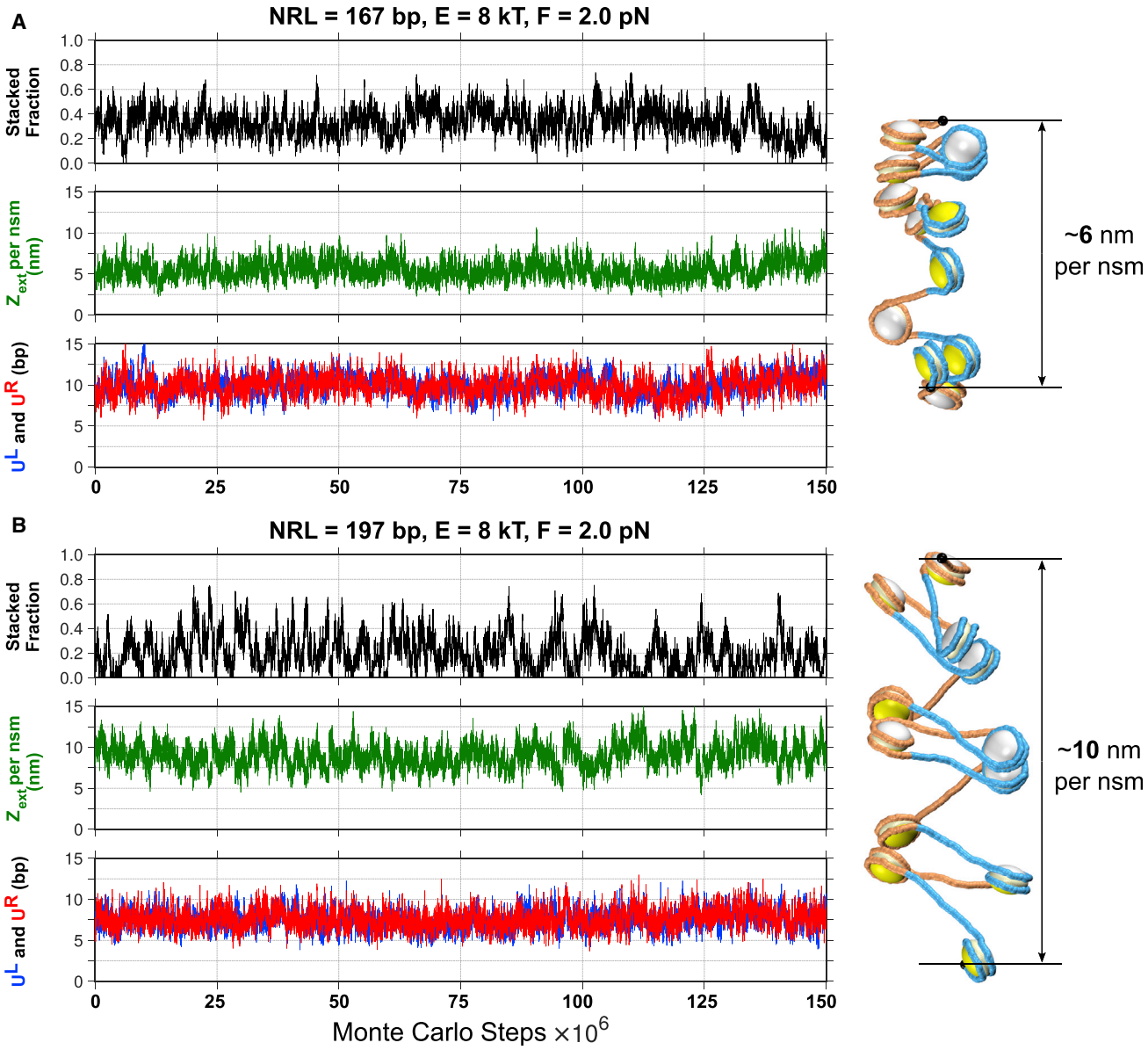

FIGURE 6 Changes in the fiber parameters during MC simulations show dynamic unwrapping and stacking of fibers. 150×10^6 MC equilibrated steps are shown for NRL = 167 bp (*A*) and 197 bp (*B*) at $F = 2$ pN. (*Top*) The fraction of stacked nucleosomes is shown. Equilibrium involves multiple stacking-unstacking transitions. (*Middle*) The extension per nucleosome is presented. The SD of extension is ~1.1 nm for NRL = 167 bp construct and ~1.4 nm for 197 bp. (*Bottom*) U^L and U^R are shown as a function of MC steps. Note that these U^L and U^R values are the averages over 12 nucleosomes in the array. Examples of the equilibrated conformations are shown on the right. Note that the structures became half open during simulations. They show the ~6-nm vs. ~10-nm extensions consistent with the experimental data (15); see Fig. 5, *A* and *B*. To see this figure in color, go online.

as a function of force, as well as statistics of U^L and U^R values for individual nucleosomes in the 12-mer arrays are shown in Fig. S8. In particular, we found that on average, unwrapping of the terminal nucleosomes is similar to that of the internal ones (Fig. S8).

Internucleosome contacts

In addition to the SF of nucleosomes, we calculated the FINI in our MC ensembles (Fig. 7). This approach is similar to the electron-microscopy-assisted nucleosome interaction capture analysis of the cross-linked nucleosome arrays made by Grigoryev et al. (38). These contact-map profiles provide important information about the relative compactness of the fiber and its morphology. For example, we observe a decrease in the FINI values if the nucleosome spacing is increased (NRL = 167 vs. 197 bp) or if an external force is applied ($F = 0$ vs. 2 pN). Naturally, an increase in the stacking energy places the distal nucleosomes in close proximity (cf. $E = 0$ with $E = 8$ kT). A decrease in unwrapping from $U = 15$ to 10 bp also results in additional interactions between the nucleosome beads.

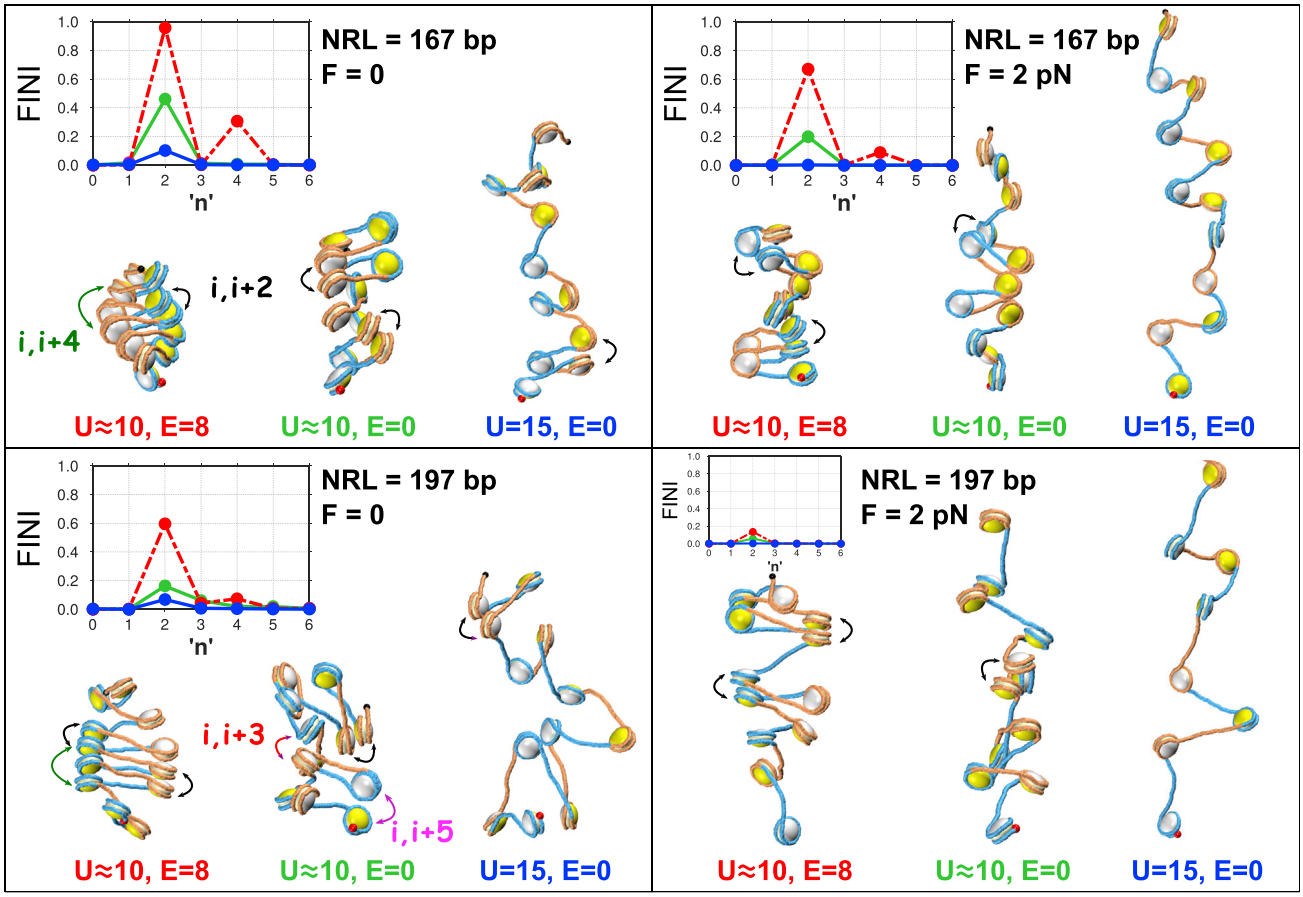

FIGURE 7 Geometry and frequency of internucleosome contacts are shown for $F = 0$ and 2 pN. The insets show the frequency of internucleosome interactions (FINI) between nucleosomes (i, $i + n$). Red indicates the interaction patterns for $E = 8$ kT and $U \approx 10$ bp, green indicates $E = 0$ and $U \approx 10$ bp, and blue indicates $E = 0$ and $U = 15$ bp. The two-start arrangement, $n = 2$, is the most frequent configuration of the fiber. Contacts between nucleosomes i and $i + 2$ are highlighted by black double-sided arrows. Rare events with $n = 3$, 4, and 5 are shown by red, green, and pink arrows, respectively. Two nucleosomes are considered to be in contact if the center-to-center distance is less than 120 Å. Details of FINI calculation are described in the Materials and Methods. To see this figure in color, go online.

The FINI contact maps show that the canonical zigzag fibers ($n = 2$) are dominant, whereas rare events of $n = 3$–5 corresponding to the three-start and five-start morphologies are also possible, albeit with much lower frequencies (Fig. 7; NRL = 197 bp, $F = 0$). In addition, the FINI profiles have peaks at $n = 4$ for $E = 8$ kT (Fig. 7). This implies that clusters of at least five stacked nucleosomes arranged in two-start zigzag conformations are relatively frequent in our MC ensembles. Of note is that recently, using single-molecule force spectroscopy, Li et al. (39) found that tetranucleosome intermediates frequently appear in nucleosomal arrays. Thus, it is tempting to speculate that our results support such transient two-start clusters of stacked nucleosomes.

DISCUSSION

We performed intensive MC simulations of unfolding of 30-nm chromatin fibers and compared the results with force spectroscopy measurements. This analysis provides detailed information about the level of compaction, range of internucleosome interactions, and dynamics of nucleosome unwrapping. Our coarse-grained model was proven successful at predicting optimal conformations and topological variability of chromatin fibers. We found a remarkable similarity between the computed optimal fiber conformations and the existing x-ray and electron cryomicroscopy structures (30). Topological variability as a function of NRL was predicted using our coarse-grained model and successfully tested experimentally (40). Recently, we found a close similarity between sedimentation velocity measured experimentally and MC simulations (41) demonstrating that our predicted conformations are likely to represent adequately the ensemble of fiber structures in vitro. Here, by adding dynamic unwrapping to that force field, we simulated oligonucleosome arrays under an external stretching force, F. Comparing the force-extension curves generated by simulations with the experimental data allowed us to elucidate the effect of different regimes of force on fiber unfolding.

Recently, Hall et al. (12) generated a detailed map of histone-DNA interactions along the DNA sequence by mechanically unzipping the DNA of single nucleosomes. By measuring the dwell times of the unzipping fork, they concluded that the terminal ~5–15 basepairs from the nucleosomal ends do not show any significant interaction with histones and thus, can unwrap easily. We translated their data into an adhesion energy profile, $G_{adh}(U)$. MC simulations utilizing this adhesion potential demonstrate that as the external force increases, the degree of unwrapping also increases. At small forces ($F = 0$–3 pN) the nucleosomes breathe by $U \approx 10$ bp at the ends. The breathing might be slightly more pronounced for short NRLs because of the stronger distortions of the linker DNA caused by the tighter packing. The breathing of the 601 nucleosomal DNA at the ends is also consistent with the accessibility of terminal 10–20 bp of nucleosomal DNA for cleavage by micrococcal nuclease (42). One can expect the end DNA breathing to be even more pronounced for natural DNA sequences because their affinity to histones is lower than in the 601 sequence (43,44).

In both constructs, with NRL = 167 and 197 bp, a plateau occurs at intermediate force $F \approx 3.5$ pN. The width of this plateau could only be explained by considerable unwrapping ($U \approx 25$–32 bp) of the nucleosomes after complete loss of stacking. Therefore, the plateau region can be interpreted as the unpeeling of the outer-turn DNA by an external force approximately equal to the adhesive force between DNA and the histone core. In other words, the height of the plateau is mostly determined by the intranucleosomal interactions in contrast to the earlier models, suggesting that the height of the plateau is defined by the strength of the internucleosome stacking (13,15,27). As follows from our MC simulations, the linear regime in the force-extension curve is entirely consistent with the dynamic stacking-unstacking of nucleosomes. This is another important difference from the existing model (15) assuming that nucleosomes are fully stacked in the linear regime.

We were also able to uncover the molecular-mechanical origin of the stochastic asymmetric unwrapping of nucleosomes observed experimentally by Ngo et al. (16). We found that it is the shape of the adhesion potential that dictates the "lopsided" opening of the nucleosome ends even if the DNA sequence is symmetric (Fig. S2). (A similar asymmetric unwrapping was observed for an asymmetric adhesion potential; data not shown). This inherent dynamic asymmetry of nucleosome revealed under external force may play a role in the nucleosome maintenance during transcription and remodeling because it has been shown that a high fraction of nucleosomes survives after being transcribed (45,46) or remodeled (47). The coordinated unwrapping-rewrapping between the two nucleosome ends may help stabilize one H2A/H2B dimer during the exchange or modification of the other dimer (48).

There is strong evidence that such mechanical asymmetry of nucleosomes may influence gene expression. The in vitro transcription studies demonstrated that nucleosomes form a polar barrier to transcriptional elongation (49,50). The molecular motors such as RNA-polymerase exert forces between 5 and 15 pN (51,52). Under these forces, the nucleosomes would unravel asymmetrically, as observed by Ngo et al. (16), thus modulating processivity of RNA-polymerase along the nucleosomal array. In addition, the stochastic and asymmetric unwrapping of nucleosomes would significantly increase the accessibility of nucleosomal DNA to transcription factors, such as p53 (53).

Regarding the internucleosomal interactions, it is generally accepted that posttranslational (epigenetic) modifications of the histone tails can significantly change the stacking and therefore alter condensation of chromatin (4,5). However, the strength of the stacking energy, E, remains a subject of debate (10–19). To the best of our knowledge, only two direct measurements of internucleosome interaction were published. Mangenot et al. (54) used osmometry and electrophoretic mobility to study the interaction between isolated nucleosome core particles (NCPs). They report a range of values between 3 and 10 kT under 100–150 mM NaCl. More recently, Funke et al. (55) integrated two nucleosomes in a DNA origami-based force spectrometer and found the free energy of stacking to be −1.6 kcal/mol. Their measurements were made at 10 mM $MgCl_2$ and cryogenic temperatures. Note, however, that the fiber stretching experiments are typically performed in the presence of no more than 1–2 mM of Mg^{2+} ions to avoid aggregation (56). Our computations suggest that the range of energies for unstacked chromatin is $E \approx 0$–3 kT, whereas $E \geq 12$ kT condenses the fiber (see representative fiber conformations for $E = 3$ (*open*), 8 (*half-open*), and 12 kT (*compact*) shown in Fig. S9). Intermediate energy values represent chromatin randomly opening and closing under thermal fluctuations. For the given force-spectroscopy settings (15), our estimate of stacking energy is $E \approx 8$ kT. The MC-simulated conformations largely resembled two-start packing, with rare events of three- to five-start morphologies. We did not observe one-start stacking folds.

Further details of the chromatin dynamics could be revealed using our current coarse-grained model with appropriate modifications. A more sophisticated DNA-histone interaction force field is essential to simulate the sequence-dependent aspects of the nucleosome dynamics in the context of long chromatin fibers. After implementing these modifications of the force field, the nucleosome breathing and sliding can be analyzed for naturally occurring DNA sequences. At the higher levels, the dynamic unfolding of fibers under fixed topology can be simulated to mimic accommodation of the DNA supercoiling during transcriptional elongation (40,57,58).

In summary, we developed a novel, to our knowledge, coarse-grained model of chromatin fiber that is consistent

with the force-extension data by Meng et al. (15) and observations of stochastic and asymmetric unwrapping of nucleosomes made by Ngo et al. (16). The force-induced gradual unwrapping accompanied by dynamic stacking-unstacking transitions account for the experimental observations (15). Our approach brings new, to our knowledge, insights into the dynamics of nucleosomal arrays, which is critical for various DNA-related cellular processes.

SUPPORTING MATERIAL

Supporting Materials and Methods, nine figures, and two videos are available at http://www.biophysj.org/biophysj/supplemental/S0006-3495(18)31007-5.

AUTHOR CONTRIBUTIONS

D.N. and V.B.Z. designed the research. D.N. developed the MC software and performed the research, then D.N. and V.B.Z. analyzed the data and wrote the article.

ACKNOWLEDGMENTS

The authors thank John van Noort from Leiden University for his invaluable comments and insights concerning this work and providing us with force-spectroscopy data. We thank George Leiman for editing the text. We are grateful to the three anonymous reviewers for their constructive critical remarks.

This work utilized the computational resources of the National Institutes of Health High-Performance Computing Biowulf cluster (http://hpc.nih.gov). Funding resources were provided by the Intramural Research Program of the National Institutes of Health, National Cancer Institute.

REFERENCES

1. Luger, K., A. W. Mäder, …, T. J. Richmond. 1997. Crystal structure of the nucleosome core particle at 2.8 A resolution. *Nature.* 389:251–260.
2. Davey, C. A., D. F. Sargent, …, T. J. Richmond. 2002. Solvent mediated interactions in the structure of the nucleosome core particle at 1.9 a resolution. *J. Mol. Biol.* 319:1097–1113.
3. van Holde, K. E. 1989. Chromatin. Springer, New York.
4. Shogren-Knaak, M., H. Ishii, …, C. L. Peterson. 2006. Histone H4-K16 acetylation controls chromatin structure and protein interactions. *Science.* 311:844–847.
5. Bannister, A. J., and T. Kouzarides. 2011. Regulation of chromatin by histone modifications. *Cell Res.* 21:381–395.
6. Lai, W. K. M., and B. F. Pugh. 2017. Understanding nucleosome dynamics and their links to gene expression and DNA replication. *Nat. Rev. Mol. Cell. Biol.* 18:548–562.
7. North, J. A., J. C. Shimko, …, M. G. Poirier. 2012. Regulation of the nucleosome unwrapping rate controls DNA accessibility. *Nucleic Acids Res.* 40:10215–10227.
8. Brehove, M., T. Wang, …, M. G. Poirier. 2015. Histone core phosphorylation regulates DNA accessibility. *J. Biol. Chem.* 290:22612–22621.
9. Andresen, K., I. Jimenez-Useche, …, X. Qiu. 2013. Solution scattering and FRET studies on nucleosomes reveal DNA unwrapping effects of H3 and H4 tail removal. *PLoS One.* 8:e78587.
10. Cui, Y., and C. Bustamante. 2000. Pulling a single chromatin fiber reveals the forces that maintain its higher-order structure. *Proc. Natl. Acad. Sci. USA.* 97:127–132.
11. Mihardja, S., A. J. Spakowitz, …, C. Bustamante. 2006. Effect of force on mononucleosomal dynamics. *Proc. Natl. Acad. Sci. USA.* 103:15871–15876.
12. Hall, M. A., A. Shundrovsky, …, M. D. Wang. 2009. High-resolution dynamic mapping of histone-DNA interactions in a nucleosome. *Nat. Struct. Mol. Biol.* 16:124–129.
13. Kruithof, M., F. T. Chien, …, J. van Noort. 2009. Single-molecule force spectroscopy reveals a highly compliant helical folding for the 30-nm chromatin fiber. *Nat. Struct. Mol. Biol.* 16:534–540.
14. Sudhanshu, B., S. Mihardja, …, A. J. Spakowitz. 2011. Tension-dependent structural deformation alters single-molecule transition kinetics. *Proc. Natl. Acad. Sci. USA.* 108:1885–1890.
15. Meng, H., K. Andresen, and J. van Noort. 2015. Quantitative analysis of single-molecule force spectroscopy on folded chromatin fibers. *Nucleic Acids Res.* 43:3578–3590.
16. Ngo, T. T., Q. Zhang, …, T. Ha. 2015. Asymmetric unwrapping of nucleosomes under tension directed by DNA local flexibility. *Cell.* 160:1135–1144.
17. Kaczmarczyk, A., A. Allahverdi, …, J. van Noort. 2017. Single-molecule force spectroscopy on histone H4 tail-cross-linked chromatin reveals fiber folding. *J. Biol. Chem.* 292:17506–17513.
18. Victor, J. M., J. Zlatanova, …, J. Mozziconacci. 2012. Pulling chromatin apart: Unstacking or Unwrapping? *BMC Biophys.* 5:21.
19. Chien, F. T., and T. van der Heijden. 2014. Characterization of nucleosome unwrapping within chromatin fibers using magnetic tweezers. *Biophys. J.* 107:373–383.
20. Katritch, V., C. Bustamante, and W. K. Olson. 2000. Pulling chromatin fibers: computer simulations of direct physical micromanipulations. *J. Mol. Biol.* 295:29–40.
21. Wedemann, G., and J. Langowski. 2002. Computer simulation of the 30-nanometer chromatin fiber. *Biophys. J.* 82:2847–2859.
22. Kepper, N., D. Foethke, …, K. Rippe. 2008. Nucleosome geometry and internucleosomal interactions control the chromatin fiber conformation. *Biophys. J.* 95:3692–3705.
23. Perišić, O., R. Collepardo-Guevara, and T. Schlick. 2010. Modeling studies of chromatin fiber structure as a function of DNA linker length. *J. Mol. Biol.* 403:777–802.
24. Collepardo-Guevara, R., and T. Schlick. 2012. Crucial role of dynamic linker histone binding and divalent ions for DNA accessibility and gene regulation revealed by mesoscale modeling of oligonucleosomes. *Nucleic Acids Res.* 40:8803–8817.
25. Dobrovolskaia, I. V., and G. Arya. 2012. Dynamics of forced nucleosome unraveling and role of nonuniform histone-DNA interactions. *Biophys. J.* 103:989–998.
26. Lequieu, J., A. Córdoba, …, J. J. de Pablo. 2016. Tension-dependent free energies of nucleosome unwrapping. *ACS Cent. Sci.* 2:660–666.
27. Kepper, N., R. Ettig, …, K. Rippe. 2011. Force spectroscopy of chromatin fibers: Extracting energetics and structural information from Monte Carlo simulations. *Biopolymers.* 95:435–447.
28. Schlick, T., J. Hayes, and S. Grigoryev. 2012. Toward convergence of experimental studies and theoretical modeling of the chromatin fiber. *J. Biol. Chem.* 287:5183–5191.
29. Clauvelin, N., P. Lo, …, W. K. Olson. 2015. Nucleosome positioning and composition modulate in silico chromatin flexibility. *J. Phys. Condens. Matter.* 27:064112.
30. Norouzi, D., and V. B. Zhurkin. 2015. Topological polymorphism of the two-start chromatin fiber. *Biophys. J.* 108:2591–2600.
31. Makde, R. D., J. R. England, …, S. Tan. 2010. Structure of RCC1 chromatin factor bound to the nucleosome core particle. *Nature.* 467:562–566.
32. Olson, W. K., A. A. Gorin, …, V. B. Zhurkin. 1998. DNA sequence-dependent deformability deduced from protein-DNA crystal complexes. *Proc. Natl. Acad. Sci. USA.* 95:11163–11168.

33. Czapla, L., D. Swigon, and W. K. Olson. 2006. Sequence-dependent effects in the cyclization of short DNA. *J. Chem. Theory Comput.* 2:685–695.

34. Metropolis, N., A. W. Rosenbluth, …, E. Teller. 1953. Equation of state calculations by fast computing machines. *J. Chem. Phys.* 21:1087–1092.

35. Kulić, I. M., and H. Schiessel. 2004. DNA spools under tension. *Phys. Rev. Lett.* 92:228101–228104.

36. Kono, H., S. Sakuraba, and H. Ishida. 2018. Free energy profiles for unwrapping the outer superhelical turn of nucleosomal DNA. *PLoS Comput. Biol.* 14:e1006024.

37. Kenzaki, H., and S. Takada. 2015. Partial unwrapping and histone tail dynamics in nucleosome revealed by coarse-grained molecular simulations. *PLoS Comput. Biol.* 11:e1004443.

38. Grigoryev, S. A., G. Arya, …, T. Schlick. 2009. Evidence for heteromorphic chromatin fibers from analysis of nucleosome interactions. *Proc. Natl. Acad. Sci. USA.* 106:13317–13322.

39. Li, W., P. Chen, …, G. Li. 2016. FACT remodels the tetranucleosomal unit of chromatin fibers for gene transcription. *Mol. Cell.* 64:120–133.

40. Nikitina, T., D. Norouzi, …, V. B. Zhurkin. 2017. DNA topology in chromatin is defined by nucleosome spacing. *Sci. Adv.* 3:e1700957.

41. Buckwalter, J. M., D. Norouzi, …, S. A. Grigoryev. 2017. Regulation of chromatin folding by conformational variations of nucleosome linker DNA. *Nucleic Acids Res.* 45:9372–9387.

42. Nikitina, T., D. Wang, …, V. B. Zhurkin. 2013. Combined micrococcal nuclease and exonuclease III digestion reveals precise positions of the nucleosome core/linker junctions: Implications for high-resolution nucleosome mapping. *J. Mol. Biol.* 425:1946–1960.

43. Bancaud, A., N. Conde e Silva, …, J. L. Viovy. 2006. Structural plasticity of single chromatin fibers revealed by torsional manipulation. *Nat. Struct. Mol. Biol.* 13:444–450.

44. De Lucia, F., M. Alilat, …, A. Prunell. 1999. Nucleosome dynamics. III. Histone tail-dependent fluctuation of nucleosomes between open and closed DNA conformations. Implications for chromatin dynamics and the linking number paradox. A relaxation study of mononucleosomes on DNA minicircles. *J. Mol. Biol.* 285:1101–1119.

45. Bintu, L., M. Kopaczynska, …, C. Bustamante. 2011. The elongation rate of RNA polymerase determines the fate of transcribed nucleosomes. *Nat. Struct. Mol. Biol.* 18:1394–1399.

46. Workman, J. L. 2006. Nucleosome displacement in transcription. *Genes Dev.* 20:2009–2017.

47. Shundrovsky, A., C. L. Smith, …, M. D. Wang. 2006. Probing SWI/SNF remodeling of the nucleosome by unzipping single DNA molecules. *Nat. Struct. Mol. Biol.* 13:549–554.

48. Yen, K., V. Vinayachandran, and B. F. Pugh. 2013. SWR-C and INO80 chromatin remodelers recognize nucleosome-free regions near +1 nucleosomes. *Cell.* 154:1246–1256.

49. Bondarenko, V. A., L. M. Steele, …, V. M. Studitsky. 2006. Nucleosomes can form a polar barrier to transcript elongation by RNA polymerase II. *Mol. Cell.* 24:469–479.

50. Kulaeva, O. I., D. A. Gaykalova, …, V. M. Studitsky. 2009. Mechanism of chromatin remodeling and recovery during passage of RNA polymerase II. *Nat. Struct. Mol. Biol.* 16:1272–1278.

51. Yin, H., M. D. Wang, …, J. Gelles. 1995. Transcription against an applied force. *Science.* 270:1653–1657.

52. Zhang, Y., C. L. Smith, …, C. Bustamante. 2006. DNA translocation and loop formation mechanism of chromatin remodeling by SWI/SNF and RSC. *Mol. Cell.* 24:559–568.

53. Cui, F., and V. B. Zhurkin. 2014. Rotational positioning of nucleosomes facilitates selective binding of p53 to response elements associated with cell cycle arrest. *Nucleic Acids Res.* 42:836–847.

54. Mangenot, S., E. Raspaud, …, F. Livolant. 2002. Interactions between isolated nucleosome core particles: A tail-bridging effect? *Eur. Phys. J. E.* 7:221–231.

55. Funke, J. J., P. Ketterer, …, H. Dietz. 2016. Uncovering the forces between nucleosomes using DNA origami. *Sci. Adv.* 2:e1600974.

56. Grigoryev, S. A., and C. L. Woodcock. 2012. Chromatin organization - the 30 nm fiber. *Exp. Cell Res.* 318:1448–1455.

57. Norouzi, D., A. Katebi, …, V. B. Zhurkin. 2015. Topological diversity of chromatin fibers: Interplay between nucleosome repeat length, DNA linking number and the level of transcription. *AIMS Biophys.* 2:613–629.

58. Wu, H. Y., S. H. Shyy, …, L. F. Liu. 1988. Transcription generates positively and negatively supercoiled domains in the template. *Cell.* 53:433–440.

Biophysical Journal, Volume *115*

Supplemental Information

Dynamics of Chromatin Fibers: Comparison of Monte Carlo Simulations with Force Spectroscopy

Davood Norouzi and Victor B. Zhurkin

Dynamics of Chromatin Fibers:
Comparison of Monte Carlo Simulations with Force Spectroscopy

Davood Norouzi and Victor B. Zhurkin
Laboratory of Cell Biology, CCR, National Cancer Institute, NIH, Bethesda, MD, USA

Supporting Materials

Energy terms and geometry

Schematic description of the DNA and fiber geometry, Monte Carlo moves, and energy terms are depicted in Figure S1.

(**I**) DNA Elastic energy. The elastic energy of the linker DNA deformation is calculated using the knowledge-based potential functions introduced by Olson et al. [32]. The stiffness constants, f_{ij}, including the cross correlations (such as Twist-Roll) are taken as averages for all 16 dinucleotides. As the rest-state values, $\bar{\theta}_i$, we use the average helical parameters of B-DNA: Twist = 34.5° and Rise = 3.35 Å.

$$E = \tfrac{1}{2} \sum_{i=1}^{6} \sum_{j=1}^{6} f_{ij}(\theta_i - \bar{\theta}_i)(\theta_j - \bar{\theta}_j)$$

(**II**) Electrostatic energy. The electrostatic energy is calculated using the Coulomb potential with 30 Å distance cutoff with charges subject to salt screening. We chose partial charges in such a way that the nucleosome remains 'slightly' negatively charged, which is consistent with electrophoresis experiments [S2]. The centers of charges considered in our calculations are: Cz, Nz in Arginine and Lysine with corresponding partial charge +1; Cd, Cg in Glutamate and Aspartate with partial charge –1, and the Phosphate (P) atoms in nucleosomal DNA with partial charge –0.3. This level of neutralization is predicted in numerical computations [S3]. The long and flexible tails of H3 histones were cut away, but their effect has been taken into account implicitly. According to recent MD simulations [S4] the

positively charged H3 tails are likely to align along the linkers, resulting in a significant neutralization of linker DNA. Linker DNA was modeled with the partial charges –0.25 per nucleotide.

We made a comparison between energy profiles obtained by the truncated Coulomb potential and the Debye-Huckel potential previously [30]. We showed that changing the details of electrostatic potential does not change quantitatively the optimal energy profiles. We chose this interaction because, in compact structures with solvent being pushed out of the crowded regions the electrostatic interactions are stronger locally and decay faster outside a cutoff range.

(**III**) Steric clashes. Steric clashes are modeled by a repulsive van der Waals potential. All the centers of charges considered above are included here, as well as the centers of the DNA base pairs (shown as gray circles in Fig. S1). The van der Waals radii are assumed to be 3.0 Å for the centers of charges and 8.0 Å for the DNA base pair centers. The potential is the repulsive part of the Lennard-Jones potential calculated as:

$$E_{vdW} = 4\varepsilon \times \sum_{i<j} \left(\frac{\sigma_i + \sigma_j}{r_{ij}}\right)^{12}$$

where ε = 2.5 kT, σ_i, σ_j are the van der Waals radii, and r_{ij} is the distance between the corresponding pseudo-atoms.

(**IV**) H4 tail – acidic patch interactions. The attractive interactions between the H4 tail and the acidic patch are modeled phenomenologically [30]. We calculate the distance, "*r*", between the H4 tail hinge, Asp24 (H4), and the patch center, Glu61 (H2A), located on two adjacent nucleosomes. The energy of the tail-patch interaction as a function of the distance is approximated by a smooth flat-well potential, where "E" defines the depth of the potential and "d = 35 Å" is the range of interaction. The energy calculated in this way corresponds to formation of one 'bridge' between two stacked nucleosomes. The optimal stacking between two nucleosomes involve two such bridges with the total energy "–E".

$$E_{tail-patch} = \frac{E}{4}\left(\frac{r-d}{1+|r-d|} - 1\right)$$

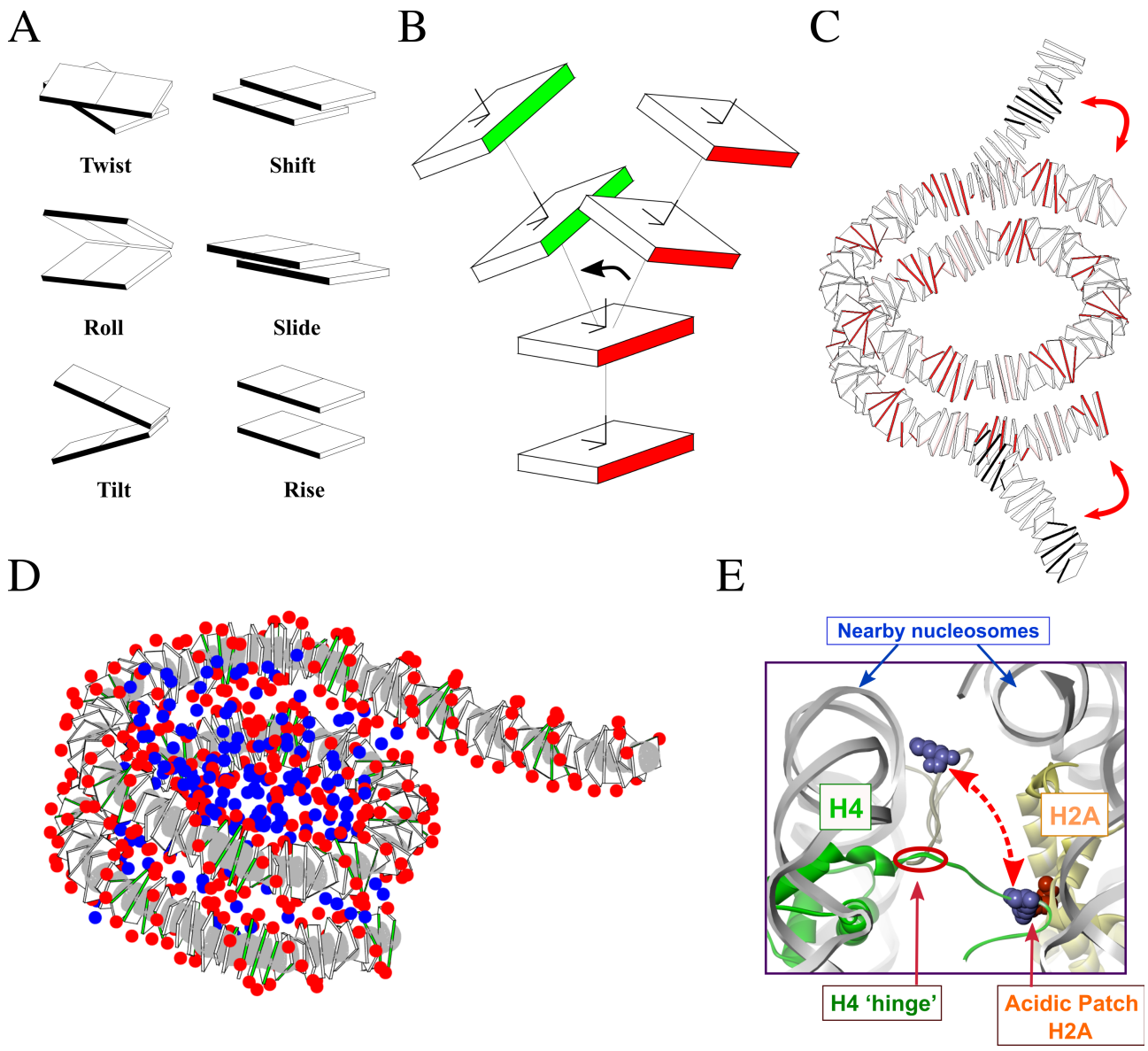

Figure S1. Schematic description of the DNA/fiber geometry, Monte Carlo moves, and energy terms. (**A**) Six base-pair step parameters define the geometry of DNA. Twist, Roll, and Tilt define the local twisting and bending of the DNA. Shift, Slide, and Rise determine the local shearing and stretching deformations (the minor groove sides of the base-pairs are shown in color). These parameters are related to the local base-pair coordinate frames according to a standard nomenclature devised in 1989 [S1]. The advantage of using this parameterization instead of utilizing only beads for the DNA is that it intrinsically includes the twist registry of the linker DNA that determines the relative orientation of the neighboring nucleosomes and the fiber topology [30], and also includes all the cross-correlation, sequence dependency, bending, and torsional flexibility terms in one single quadratic energy equation

[32]. The quadratic nature of this energy also allows us to initialize the conformation of the fiber using Gaussian sampling method [33].

(**B**) A typical Monte Carlo (MC) move is shown here. Six base-pair step parameters are updated in each move. The geometry of the linker DNA fluctuates around the regular B-DNA. The regular B-DNA parameters are [Twist, Tilt, Roll, Shift, Slide, Rise] = [34.5°, 0, 0, 0, 0, 3.35 Å] on average. In each MC step one base-pair step in one of the linkers (which include the unwrapped part of the nucleosomes (**C**) as well as the linker) is selected and the base-pair step parameters are changed randomly in the range of [δTwist, δTilt, δRoll, δShift, δSlide, δRise] = [±5°, ±3°, ±5°, ±0.3Å, ±0.5Å, ±0.2Å]. The range of values are chosen based on the rigidity matrix of deformations for DNA [32] to produce ~40% success rate for the MC step updates. The entire fiber "down-stream" of this change goes through a rigid body motion. In this figure, the second base-pair step is changed (as highlighted by the arrow). Thereby, the first two base pairs remain intact while the upper part is moved in space by some rotation and translation.

(**C**) Two nucleosome conformations, one with no unwrapping (red minor grooves) and one with U = 15 bp (black minor grooves) are shown. Unwrapping adds extra flexibility and extensibility to the fiber.

(**D**) To calculate electrostatic and van der Waals interactions, positive charges on arginines and lysines are considered (blue balls) as well as negative charges on aspartates, glutamates, and DNA phosphates (shown in red). All charges were partially neutralized to mimic the salt screening effects [30]. Large gray spheres assigned to the center of each base-pair are additional 'virtual' neutral atoms introduced to avoid the steric clashes with the DNA. After changing the base-pair step parameters and their local coordinate frames in each MC step, positions of the histones, centers of base pairs, and the phosphates are updated.

(**E**) During the course of simulations multiple stacking or H4 tail – acidic patch bonds are formed or broken down as nucleosomes change their relative surface to surface distance [30]. The depth of the potential is determined by the parameter "E" (see above).

Figures (A) to (D) are generated using MATLAB and figure (E) is generated by Accelrys Discovery Studio software.

Adhesion energy profile

In this section we derive a profile for the free energy of unwrapping, $G_{adh}(U)$, based on available force-spectroscopy data. Using dynamic force spectroscopy, Brower-Toland *et al.* [S5] estimated the free energy of unwrapping of the outer turn of DNA (U = 38 bp) as ~12 kcal/mol = 20 kT. Assuming that the adhesion energy is distributed uniformly over DNA, the energy per base pair is 0.26 kT/bp. This is consistent with the overall formation energy of nucleosomes estimated to be ~42 kT for 147 bp [S6] which gives the average adhesion energy per base pair ~0.28 kT/bp (Figure S2, red line).

To elucidate a detailed map of histone-DNA interactions along the DNA sequence with high precision, the mechanical unzipping of DNA from a single nucleosome 601 has been done by Hall *et al.* [12] using optical tweezers. The idea behind these experiments is that the dwell times measured at different DNA positions reflect the strengths of histone-DNA interactions at those positions. However, translating these dwell times into adhesion energy values is not straight-forward.

By treating the dwell times of DNA unwrapping measured by Hall *et al.* [12] as a Markov chain process, Forties *et al.* [S7] obtained an estimate for the adhesion energy landscape (black profile in Figure S2). For the initial stage of DNA unwrapping, $U \leq 28$ bp, they find the adhesion energy per base pair ~0.05 kT/bp (slope of the black curve at small U). The reason for this very small value is that Forties *et al.* chose the dwell time profile of the unzipping fork measured at the very high force F = 28 pN (Fig. 2 in [12]), with the dwell times being undetectable at the nucleosome ends. Their energy values are very low and predict a much more open '601' nucleosome than follows from Meng *et al.* force extension data [15] (simulation results with Forties *et al.* potential not shown).

Therefore, to estimate the adhesion energy of DNA, we used the unzipping traces measured at lower forces with the non-zero dwell times at the nucleosome ends (Fig. 3b in [12]). Our approach is based on the following assumptions: (1) Local unwrapping rate k_u is proportional to the inverse of the dwell time and relates to the adhesion energy, G_{adh}, by a Boltzmann factor: $k_u = 1/\tau = k_0 \exp(-G_{adh})$. (2) The rate constant k_0 is chosen so that the energy of unwrapping for the half of nucleosome (ΣG_{adh}) is ~20 kT [S6]. (3) If the dwell times are undetectable ($\tau \sim 0$) for certain DNA regions, we assign a minimum energy $G_{adh}^{min} = 0.13$ kT/bp, which is a half of the average adhesion value (see above).

Based on these assumptions, we calculated the green profile shown in Figure S2, which was used as the adhesion energy function, $G_{adh}(U)$, in our computations. This potential function allows the nucleosome ends to fluctuate between U = 0 and 20 bp at small forces F < 4 pN, with the average U varying between 8 and 15 bp depending on the external force (see Figures 5 and S8).

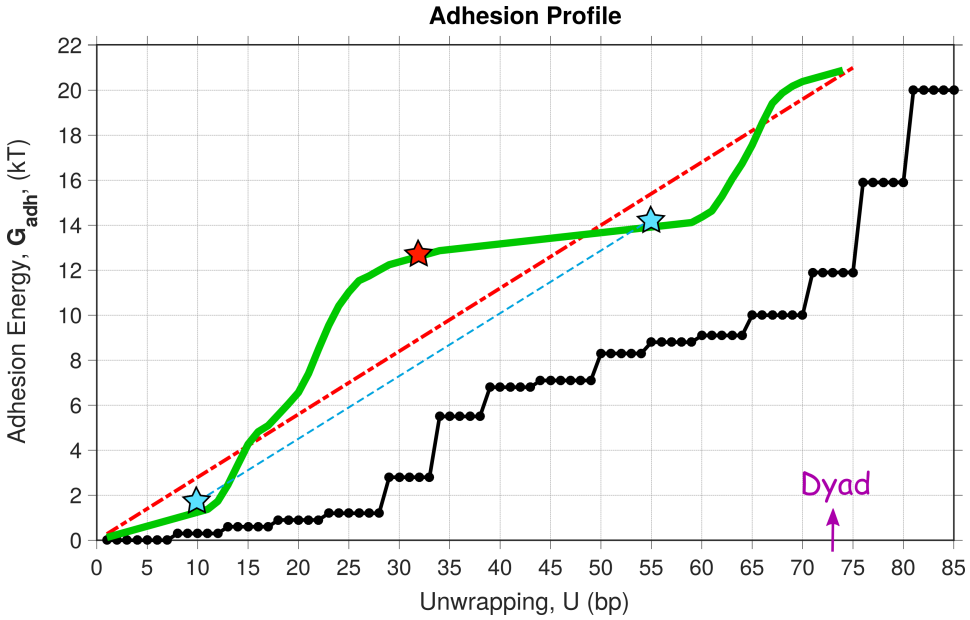

Figure S2: Adhesion energy as a function of nucleosomal DNA unwrapping. **Red**: Linear profile representing the average DNA-histones interactions (the slope 0.28 kT/bp). **Black**: Forties *et al.* [S7] translated the dwell time histogram obtained at high force F = 28 pN (Fig. 2 by Hall *et al.* [12]) into adhesion energy by implementing a Markov chain model. **Green**: Our estimate based on the average dwell times measured at low forces (presented in Fig. 3b by Hall *et al.* [12]). Importantly, this profile is lower than the average energy G_{adh} (red line) at some levels of unwrapping, while higher in other regions. By contrast, the Forties *et al.* profile remains lower than $G_{adh}(U)$ for any unwrapping U.

The curvature changes sign in the non-linear green profile. Notably, its central fragment locally concaves downward. This means that the central part of the graph lies above a line segment, dashed cyan, connecting the end points. This is important for understanding the structural origin of the bifurcation effect observed at high external forces $F \geq 4$ pN, when the average value $U = (U^L + U^R) / 2$ increases up to ~30 bp (Figures 5C and 5D).

Consider the following example. Let us assume that $(U^L + U^R) = 64$ bp. If the DNA unwrapping at both left and right ends of nucleosome is the same, $U^L = U^R = 32$ bp, the total adhesion energy is ~25 kT (which is two times the energy at the red asterisk shown in Figure S2). If, however, $U^L = 10$ bp and $U^R = 54$ bp, the total energy is ~16 kT (sum of the energies at the cyan asterisks shown in Figure S2). This simple example explains why it is more favorable to have a strong unwrapping $U \approx 55$ bp at one end, rather than to have 'intermediate' unwrapping $U \approx 30$ bp at the both ends of a nucleosome.

The region of steep increase in the adhesion energy (U = 15 – 25 bp) corresponds to the DNA positions where the arginines deeply penetrate into the minor groove of nucleosomal DNA [S8-S9]. Strong asymmetric unwrapping ensures that only one end of the nucleosome (the side with U ≈ 55 bp) pays to climb this energy barrier while the symmetric unwrapping requires twice as much energy. Importantly, as explained in the main manuscript, symmetric and asymmetric conformations generate similar Z_{ext} values.

In summary, the bimodal distribution of DNA unwrapping ($U^L \neq U^R$) helps decreasing the total adhesion energy under strong extension. In turn, this bimodality is a consequence of the specific shape of the adhesion energy profile, namely, its downward curvature at U ≈ 25 bp.

Simulation of unwrapping-rewrapping dynamics

Below, we describe the MC procedure used for simulation of spontaneous unwrapping-rewrapping of nucleosomal DNA. The nucleosome core particle is assumed to be fixed except for the unwrapped DNA, which is treated as a part of the "dynamic linker" DNA. The numbers of unwrapped base pairs at the Left and Right ends of a nucleosome are denoted U^L and U^R respectively (see the numbering scheme in Figure S3-A). The linker DNA is modeled at the level of base pairs and dimeric steps, and its trajectory is described by six dimeric step parameters [30, 32]. The dimeric steps and the base pairs are numbered in a conventional way, so that the step [i] describes transition from base pair (i) to base pair (i+1) [S1, 32].

In a single Monte Carlo step, we choose randomly a dynamic linker L_i (connecting nucleosomes N_i and N_{i+1}). Then, a dimeric step is selected from the following list of steps:

[145 – U^R – 1], **[145 – U^R]**, [145 – U^R + 1], …, [145], … [NRL], [1], [2], … **[U^L]**, **[U^L + 1]**

Here, the underlined steps belong to nucleosome N_{i+1}. The steps shown in magenta and blue are denoted in Figure S3-B by magenta and blue arrows, respectively. The magenta color indicates possible additional DNA unwrapping, while the blue color means that we either randomly change conformation of this dimeric step, or we perform a rewrapping move.

These are the three possible moves:

– (**Normal move**) If the selected dimeric step is not magenta or blue, its helical parameters are changed by the "six random increments" described in the Methods section and Figure S1. This move and the other ones (described below) include updating configuration of the nucleosome array, computing the "new" energy and performing the Metropolis acceptance test.

– (**Unwrapping move**) If the magenta dimeric step is selected, it is treated as the "newly unwrapped step". The helical parameters of this step are built using "six random increments" with the equilibrium B-DNA conformation as the starting point. If the new fiber conformation is accepted during the Metropolis test, then for the corresponding nucleosome

$$U^R \rightarrow U^R + 1 \quad \text{or} \quad U^L \rightarrow U^L + 1.$$

– (**Rewrapping move**) When the blue dimeric step is selected, it is treated as the "potentially rewrapping boundary step." With probability 50% it undergoes the "normal move" change, otherwise it rewraps (around the histone core). Rewrapping means restoring the helical parameters of DNA in the template nucleosome 601 in that position. Elastic energy of the newly wrapped DNA step is set to be zero. If the new fiber conformation is accepted, then for the corresponding nucleosome

$$U^R \rightarrow U^R - 1 \quad \text{or} \quad U^L \rightarrow U^L - 1.$$

The total adhesion energy of every nucleosome, $G_{adh}(U^R_i) + G_{adh}(U^L_i)$, is added to the total energy.

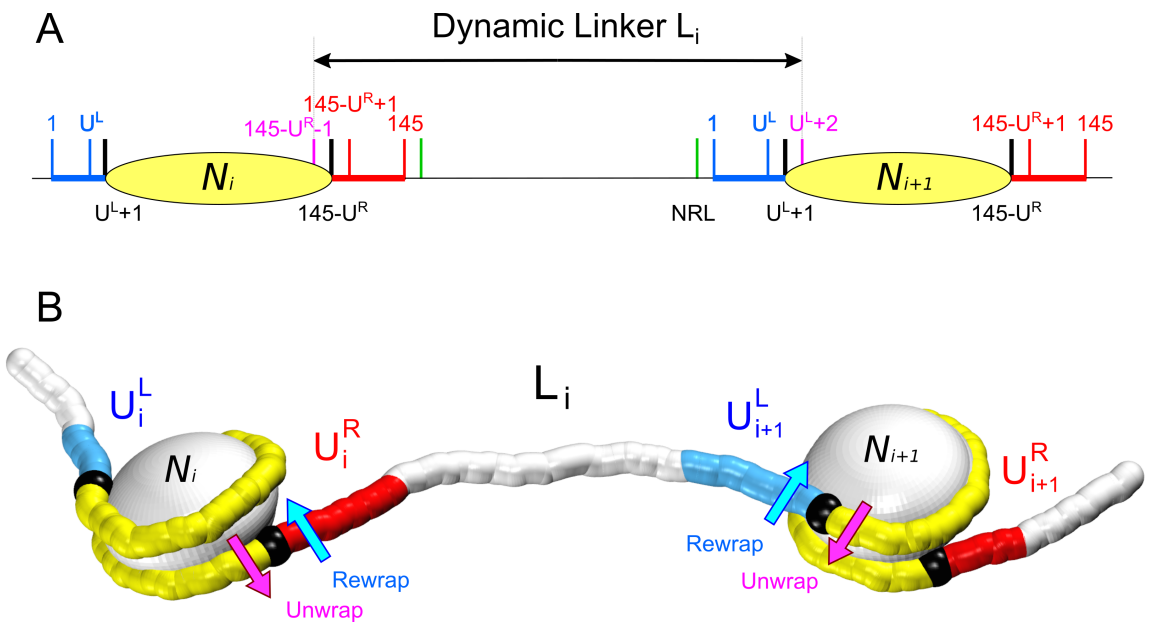

Figure S3: Schematic presentation of Monte Carlo procedure including dynamic unwrapping-rewrapping of nucleosomal DNA.

(A) Scheme explaining numbering of DNA base pairs. At the Left end, the base pairs 1, 2, … U^L are unwrapped; they are shown in blue. Similarly, at the Right end, the base pairs $145\text{-}U^R+1$, … 145 are unwrapped; they are shown in red. The yellow ovals represent DNA attached to histones; the boundary base pairs U^L+1 and $145\text{-}U^R$ are shown in black.

(B) Two adjacent nucleosomes N_i and N_{i+1} connected by dynamic linker L_i. The DNA attached to the histone core is shown in yellow, with the boundaries in black (consistent with (A)). The DNA unwrapped at the Left and Right ends of nucleosomes is colored in blue and red, respectively. The magenta arrows indicate additional DNA unwrapping, while the blue arrows denote a rewrapping move.

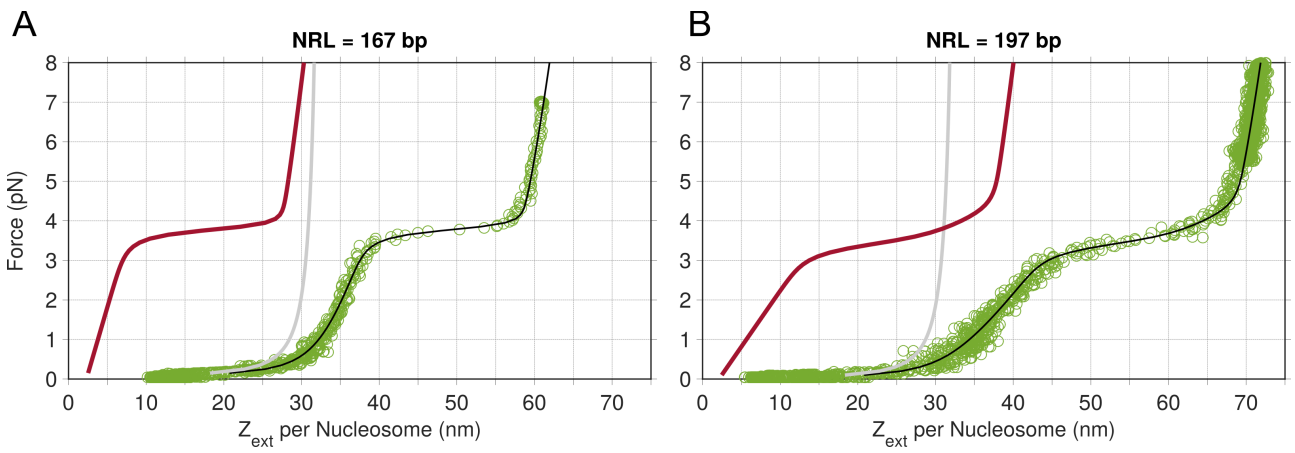

Figure S4. Extracting the force-extension response of the nucleosome arrays from raw experimental data kindly provided by J. van Noort (green circles). The force-spectroscopy measurements were performed by Meng *et al.* [15] for DNA containing 30 × 167 bp (A) and 15 × 197 bp repeats (B) of the Widom '601' nucleosome positioning sequence. To fit the data (which are normalized per nucleosome) we used the four-state model of chromatin fibers developed by Meng *et al*. [15]. The fitted curves are shown in black. The experimental setting involves 2035 bp-long DNA handles holding the nucleosome array between the surface of the flow cell and the magnetic bead. Note that, in practice with certain amount of free DNA attached to the flow cell surface or the magnetic tweezer bead, and several tetrasomes assembled on the handles, the effective length of the free DNA is considerably less than 2035 bp. The free DNA handles' response to the external force was estimated with a worm like chain (WLC) model, with the persistence length of 50 nm using the Meng *et al.* multi-state model [15]. Subtracting the WLC component (gray curves) from the black curves gives us the brown curves representing the net response of the nucleosome arrays.

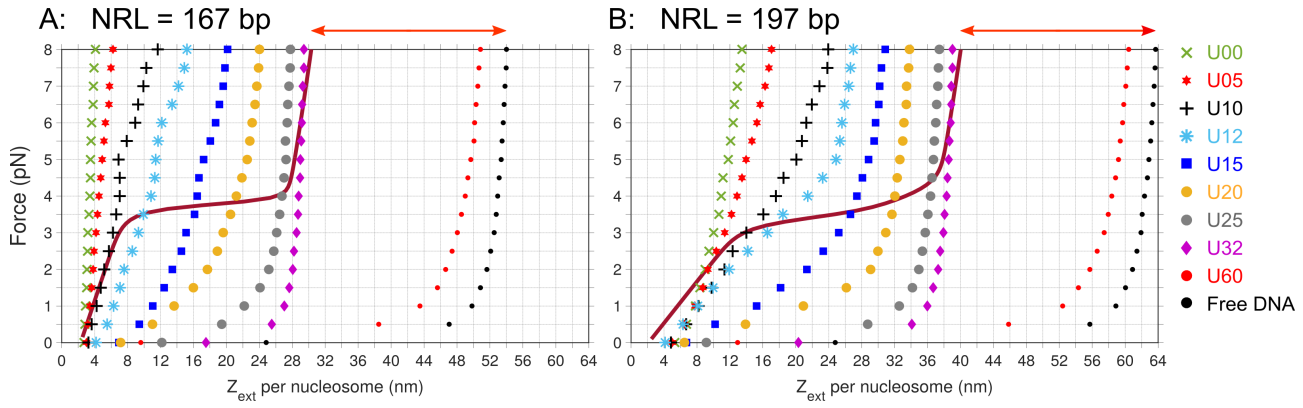

Figure S5. The force-extension profiles for the fibers with NRL = 167 bp (A) and 197 bp (B) obtained for different uniform unwrapping of nucleosomes, U, varying from 0 to 72 bp, and the stacking energy E = 0. The dotted lines (with various symbols) represent average extension per nucleosome obtained from MC simulations. The solid curves show experimental data [15]. This figure includes the data of Figure 2 plus U = 5, 60, and 72 bp cases. The red arrows represent the difference in Z_{ext} between U = 32 bp and U = 72 bp (free DNA): the 24 ± 1.0 nm extension corresponds to the inner-turn unwrapping of nucleosomes (F = 8 pN, NRL = 167 and 197 bp). This is very close to the values measured by Meng *et al*., 24 ± 8 nm and 24 ± 7 nm for NRL = 167 and 197 bp, respectively [15]. At small U and small force the force-extension curve is linear while at U = 25 – 72 bp, the force-extension dependence resembles a WLC polymer response.

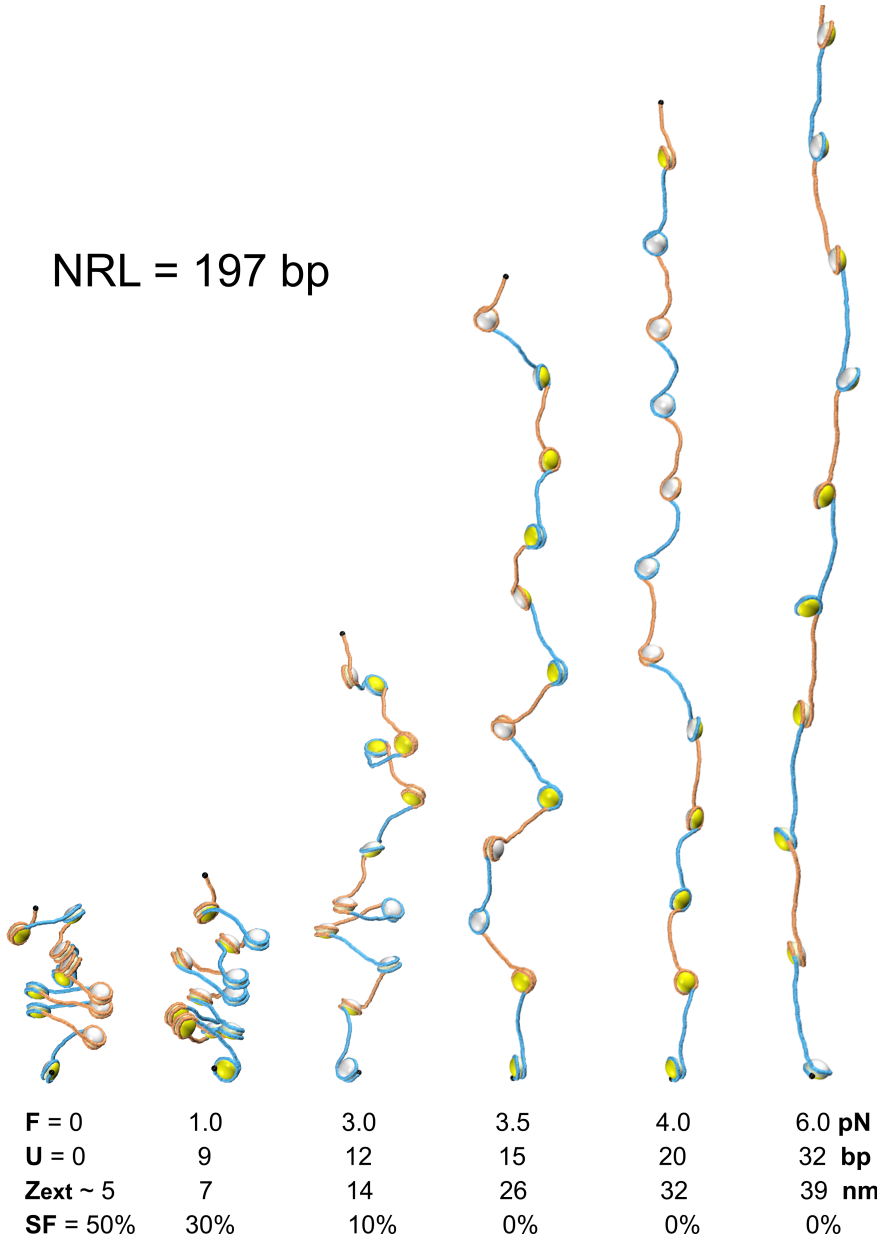

Figure S6. Typical conformations of the chromatin fiber with NRL = 197 bp simulated for the external force increasing from F = 0 to 8 pN. At small forces F ≤ 3.0 pN the DNA unwrapping is insignificant, U ≤ 12 bp, and the fiber remains relatively compact despite numerous stacking-unstacking events. With the increase in applied force, the unwrapping of nucleosomal DNA becomes much stronger and goes up to U = 20 bp at F = 4 pN, and up to U = 32 bp at F = 8 pN. These MC simulations were performed for the stacking energy E = 8 kT. At F = 3.5 pN and higher, the inter-nucleosome stacking is lost completely. The force-unwrapping, force-extension, and force-unstacking dependencies are presented at the bottom. See also the Supplementary Movies.

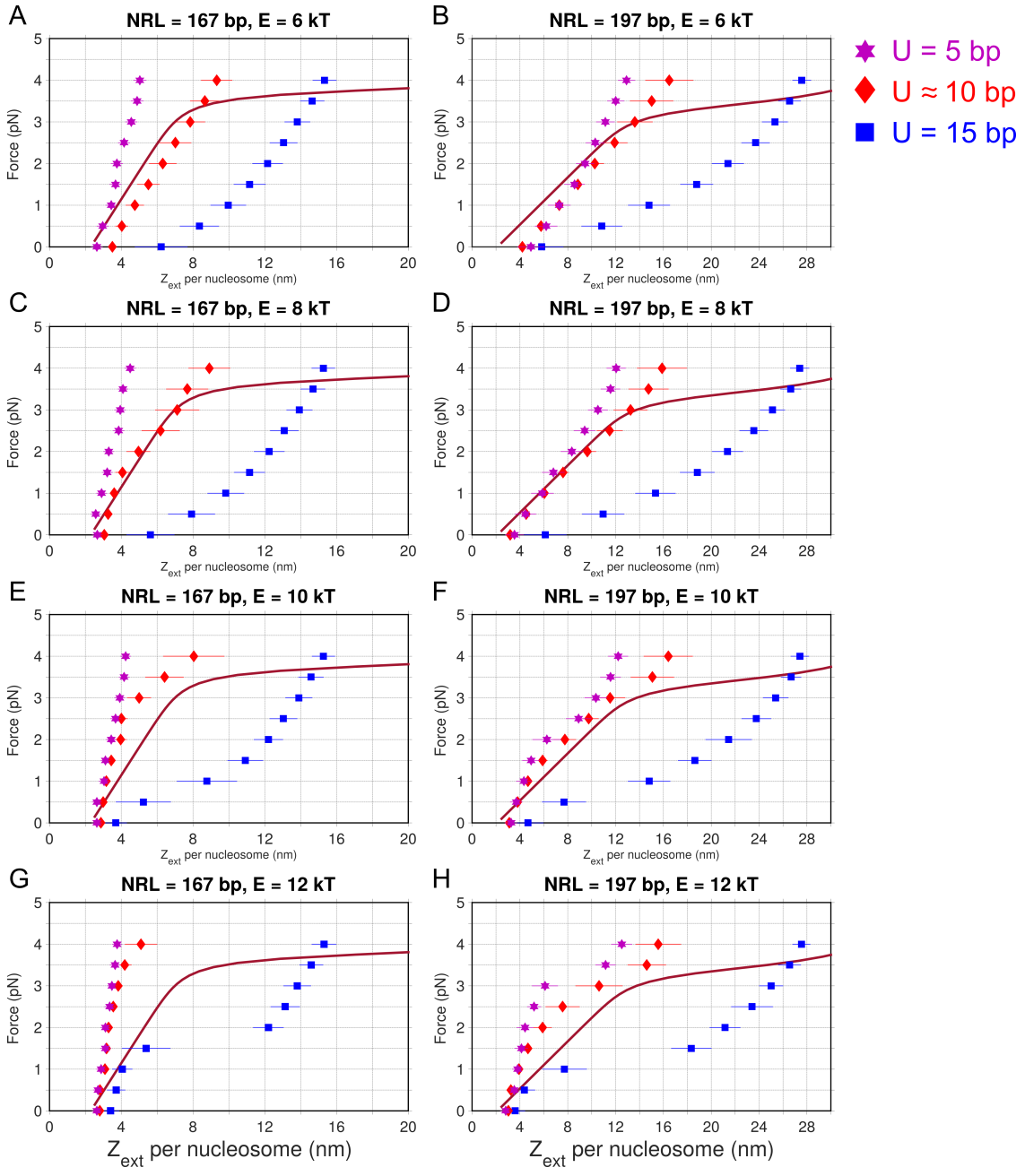

Figure S7. Selecting the optimal parameters (unwrapping, U, and stacking energy, E) accounting for the experimental observations (solid lines). In our MC simulations, we systematically changed U from 5 to 15 bp and E from 6 to 12 kT for both NRL = 167 and 197 bp. The fibers with U = 15 bp are excluded from further consideration since they do not show a linear behavior at small forces (A, B: E = 6 kT and U = 15 bp) and increasing the stacking energy does not produce the stable linearity we seek (G, H: E = 12 kT and U = 15 bp). Stacking energy E = 6 kT is too low and cannot generate the

experimentally observed extensions for NRL = 197 bp (B). Stacking energy E = 12 kT is too high and no MC calculated curves coincide with the experiment (G, H). Stacking energy E = 10 kT is too high for NRL = 167 bp (E). Thus, we find that E = 8 kT is the optimal energy value: it stabilizes a linear regime with U ≈ 10 bp (more specifically, U = 10 – 12 bp for NRL = 167 bp and U = 9 – 12 bp for NRL = 197 bp, at F ≤ 3.0 pN). To reach the observed extensions in the plateau region, nucleosomes must unfold beyond this initial unwrapping at intermediate forces. All stacks are disrupted at force F = 3.5 – 4.0 pN, and unwrapping U increases from 12 to 25 bp in this force regime.

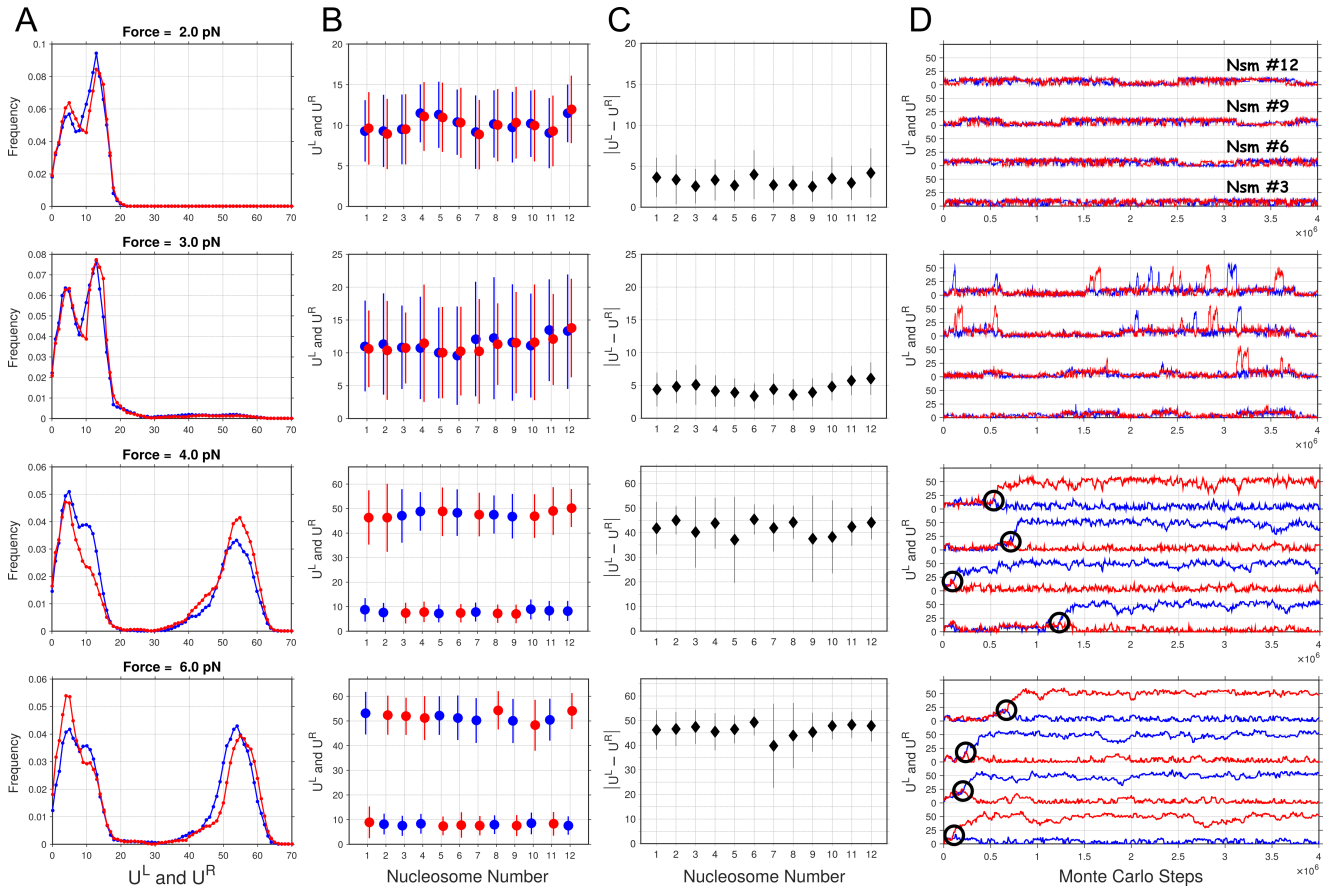

Figure S8. Spontaneous unwrapping of nucleosomal DNA during MC simulations.

The data are presented for the 167 × 12 nucleosome array; external force varies from 2.0 to 6.0 pN.

Column (A). The histograms for DNA unwrapping at the left and right ends of nucleosomes, U^L (blue) and U^R (red), are shown. At forces below 4.0 pN, the DNA unwrapping mostly remains within a narrow interval from 0 to 20 bp. At forces $F \geq 4.0$ pN, the distribution of DNA unwrapping becomes bimodal, with one peak corresponding to the U^L and U^R values less than 20 bp, and the second peak, to unwrapping of 55 (±10) bp. This bifurcation occurs due to the locally concave profile of the adhesion potential (Figure S2).

Column (B). The averages and fluctuations of U^L and U^R for 12 individual nucleosomes are presented. At the forces F = 2.0 and 3.0 pN, for each nucleosome the U^L and U^R values are nearly identical. The unwrapping is somewhat stronger for the terminal nucleosomes #1 and #12 (compared to the internal nucleosomes #2 to #11), but this difference of ~2 bp is insignificant. At F = 3.0 pN, the fluctuations of U^L and U^R are higher than at F = 2.0 pN, which is consistent with occasional DNA unwrapping (up to 55 bp) observed at F = 3.0 pN. At the forces F = 4.0 and 6.0 pN, the two sets of the U^L and U^R values correspond to the two unwrapping branches presented in the histograms.

For example, at F = 6.0 pN, in nsm #3 and nsm #12 the red circles and bars (U^R) are on the top, indicating that the unwrapping occurred at the right ends of these nucleosomes. Accordingly, in the right panel, in nsm #3 and nsm #12 the red trajectories are on the top.

On the other hand, in nsm #6 and nsm #9 the blue circles (U^L) are on the top, which is consistent with the blue trajectories #6 and #9 being on the top in the right panel.

Column (C). The absolute difference between U^L and U^R for individual nucleosomes is a direct measure of unwrapping asymmetry. The ensemble averages and standard deviations of $|U^L - U^R|$ values for all nucleosomes in the 12-mer array are presented here. At low forces, $F \sim 0 - 3$ pN, the asymmetry of unwrapping does not exceed 4 – 5 bp. At $F \geq 4.0$ pN, this value increases up to 40 – 45 bp.

Column (D). The trajectories visualizing evolution of the U^L and U^R values during the first 4 million MC steps are presented for selected nucleosomes (#3, #6, #9 and #12). Consistent with the histograms on the left, at forces $F < 4.0$ pN, the U^L and U^R values fluctuate between 0 and 20 bp. Rare occurrences of strong DNA unwrapping (up to 55 bp) in isolated nucleosomes are observed at F = 3.0 pN. At forces $F \geq 4.0$ pN, the trajectories divide in two branches – one remains between 0 and 20 bp, and the other goes up to 40-60 bp. The bifurcation points are emphasized by the black circles.

In summary, U^L and U^R, fluctuate independently and branch off at high forces. We don't observe any cooperativity in the asymmetric unwrapping of neighboring nucleosomes, that is, the left and right arms of adjacent nucleosomes unwrap independently. This reflects the stochastic nature of the nucleosome opening.

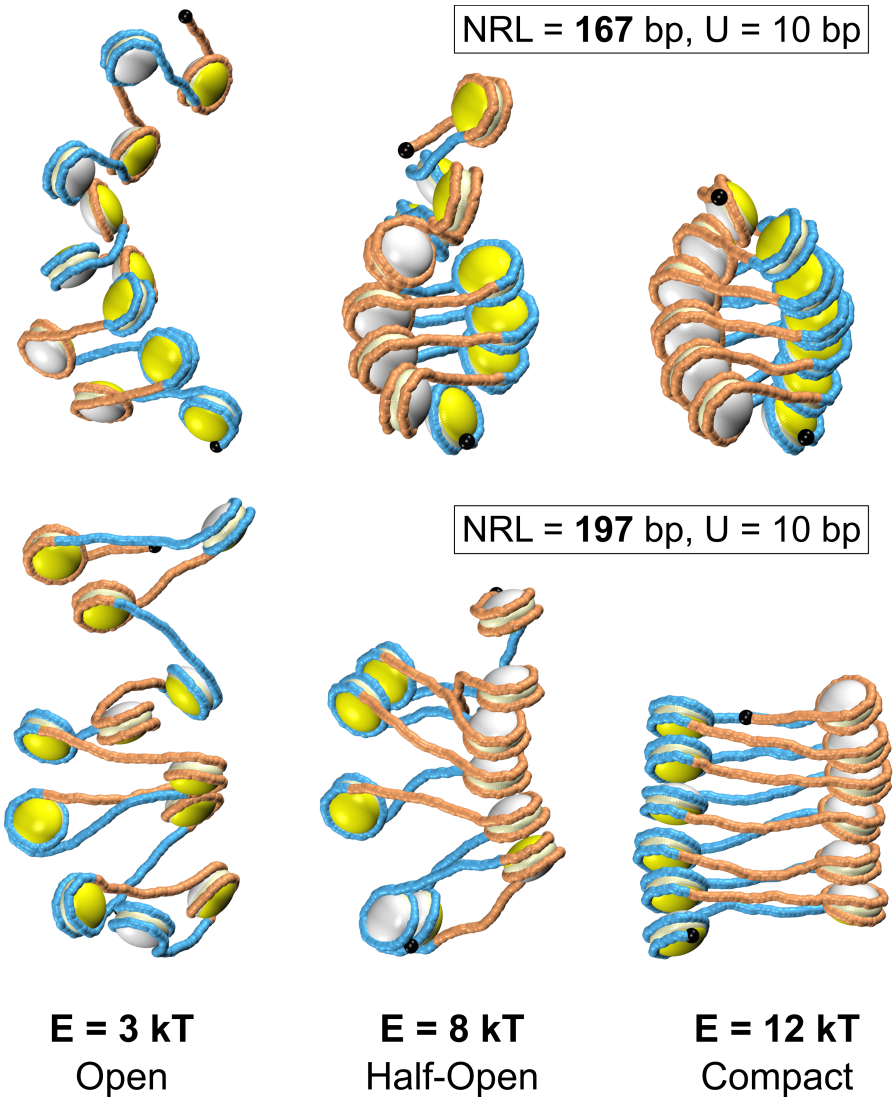

Figure S9. Representative fiber conformations for E = 3 kT (open), 8 kT (half-open), and 12 kT (compact) are shown at zero external force. The MC-simulated conformations largely resembled two-start packing, with rare events of three- to five-start morphologies. We don't observe solenoid (one-start) stacking folds. Our computations suggest that the range of energies for unstacked chromatin is E ≈ 0 – 3 kT, while E ≥ 12 kT condenses the fiber. Intermediate energy values, E ≈ 8 kT, represent chromatin randomly opening and closing under thermal fluctuations.

References:

S1. Dickerson, R. E., M. Bansal, C. R. Calladine, …, A. H. -J. Wang, and V. B. Zhurkin. 1989. Definitions and nomenclature of nucleic acid structure parameters. *EMBO J*. 8:1-4.

S2. Hewish, D. R. and L. A. Burgoyne. 1973. Chromatin sub-structure. The digestion of chromatin DNA at regularly spaced sites by a nuclear deoxyribonuclease. *Biochem Biophys Res Commun.* 52:504-510.

S3. Materese, C. K., A. Savelyev, and G. A. Papoian. 2009. Counterion atmosphere and hydration patterns near a nucleosome core particle. *J Am Chem Soc.* 131:15005-15013.

S4. Shaytan, A.K., G.A. Armeev, A. Goncearenco, V.B. Zhurkin, D. Landsman , and A.R. Panchenko. 2016. Coupling between histone conformations and dna geometry in nucleosomes on a microsecond timescale: atomistic insights into nucleosome functions. *JMB*. 428:221-237.

S5. Brower-Toland, B. D., C. L. Smith, R. C. Yeh, J. T. Lis, C. L. Peterson, and M. D. Wang. 2002. Mechanical disruption of individual nucleosomes reveals a reversible multistage release of DNA. *Proc. Natl. Acad. Sci. U.S.A.* 99:1960-1965.

S6. Ranjith, P., J. Yan , and J. F. Marko. 2007. Nucleosome hopping and sliding kinetics determined from dynamics of single chromatin fibers in xenopus egg extracts. *Proc Natl Acad Sci USA*. 104:13649.

S7. Forties, R. A., J. A. North, S. Javaid, O. P. Tabbaa, R. Fishel, M. G. Poirier, and R. Bundschuh. 2011. A quantitative model of nucleosome dynamics. *Nucleic Acids Research*. 39:8306-8313.

S8. Rohs, R., S. M. West, A. Sosinsky, P. Liu, R. S. Mann, and B. Honig. 2009. The role of DNA shape in protein-DNA recognition. *Nature*. 461:1248.

S9. Wang, D., N. B. Ulyanov, and V. B. Zhurkin. 2010. Sequence-dependent Kink-and-Slide Deformations of Nucleosomal DNA Facilitated by Histone Arginines Bound in the Minor Groove. *J. Biomol. Struct. Dyn*. 27:843-859.